Volume 80_2 (2022) 129-153

boletim paranaense de Geociências
ISSN: 0067-964X

U-PB AND LU-HF IN ZIRCON DECIPHERING MAGMATIC PULSES OF THE JUÍNA KIMBERLITE: IMPLICATIONS FOR THE LITHOSPHERIC MANTLE ISOTOPIC COMPOSITION OF THE AMAZONIAN CRATON

MARCO HELENIO DE PAULA ALVES COELHO[1], MARIA VIRGINIA ALVES MARTINS[2], ARMANDO DIAS TAVARES JR.[1], LETICIA MUNIZ[1], LUIZ FELIPE ROMERO[1], GABRIEL ALVES PAIVA[1], WILLIAN GIOVANI ZAN[3], RICARDO KALIKOWSKI WESKA[3], MAURO CESAR GERALDES[1]

1 Universidade Estadual do Rio de Janeiro (UERJ), Laboratório Multiusuário de Meio Ambiente e Materias (MULTILAB). Rua São Francisco Xavier 524, sala 3107F Maracanã, Rio de Janeiro-RJ - CEP 20550-013. E-mail: marco.helenio@gmail.com; tavares.armandodias@gmail.com; let.muniz03@gmail.com; romerolipe@gmail.com; gabialvespaiva13@gmail.com; mauro.geraldes@gmail.com

2 Universidade de Aveiro, Campus de Santiago. 3810-193 Aveiro, Portugal. E-mail: virginia.martins@ua.pt

3 Universidade Federal de Mato Grosso, Departamento de Recursos Minerais. Av. Fernando Corrêa da Costa 2367 Boa Esperança, Cuiabá – MT – CEP 78060-900. E-mail: willianzan@gmail.com; rweska@ufmt.br

Abstract - *This work aims to analyze U-Pb and Lu-Hf ages in zircons formed together with diamonds from the kimberlite province of Juína, in Mato Grosso state, Brazil. Fourteen megacryst (2-3 cm) of zircon were imaged by cathodoluminescence to evaluate the internal structure of the zircon grains and zoning features related to structures of reactions and resorption indicative of magma mixture during evolution. According to the taken images, most of the investigated crystals have a non-metamict structure, with rare fractures, inclusions, and overgrowths, which generates a small degree of heterogeneity. Analyses by Laser Ablation- Multi-Collector- Inductively Coupled Plasma Mass Spectrometry (LA-MC-ICP-MS) were performed to determine grain ages. Concordia diagrams indicate ages ranging from 99.8 ± 1.6 Ma to 89.5 ± 5.6 Ma with two clusters indicating different magmatic pulses. The analyzed zircons displayed total concentrations of U and Th ranging from 108 to 673 mg kg-1 and 26 to 194 mg kg-1, respectively, and U/Th values varying between 4 and 0.3. The concentrations of U and Pb suggest the occurrence of magmas with two distinct signature components. One hundred and twenty Lu-Hf isotopic results obtained by LA-MC-ICP-MS indicate homogeneity in the isotopic composition, with εHf values ranging from +2.2 to -1.9, and depleted mantle model ages (TDM) between 1.45 Ga and 2.55 Ga. The results suggest that the kimberlite magma derives from a mantle source enriched with an Hf isotopic signature equivalent to the chondritic unfractionated reservoir (CHUR).*

Keywords*: U-Pb Geochronology; Lu–Hf analysis; LA-MC-ICP-MS; Zircon; Kimberlite; mantle sources*

Citação*: COELHO, M. H. P, MARTINS, M. V. A., TAVARE JR., ARMANDO DIAS, MUNIZ, L. ROMERO, L. F. R., PAIVA, G. A., ZAN, W. G., WESKA, R. K. GERALDES, M. C. U-Pb and Lu-Hf in zircon deciphering magmatic pulses of the Juína Kimberlite: Implications for the lithospheric mantle isotopic composition of the Amazonian Craton. Boletim Paranaense de Geociências, v. 80, n.2, p. 129-153. 2022.*

boletim paranaense de Geociências
ISSN: 0067-964X

1. INTRODUCTION

Mato Grosso state (MT; midwestern Brazil), with 117 kimberlite intrusions, has the second largest number of bodies with known kimberlitic affinity. With few isolated intrusions, these rocks are preferably grouped into four kimberlite fields, namely Juína, Paranatinga, Traíra and Jauru (Fig. 1). Three kimberlite bodies, called Traíra-2, 3 and 6, are located in the southeast of the Amazonas state and close to the border with Mato Grosso state (Teixeira et al., 1998a, b; Kaminsky et al., 2010).

The Juína Kimberlite Field is the most important in terms of the amount of kimberlite bodies (Fig. 1) and diamond potential, according to data so far known (e.g. Davis et al., 1977; Heaman et al., 1998; Kaminsky et al., 2010). It is located in the NW of the Mato Grosso state (MT), SW of the city of Juína, and consists of 52 bodies, which according to Davis et al. (1977), Teixeira et al. (1996), Heaman et al. (1998) and Kaminsky et al. (2010) have ages ranging between 79.2 and 94.6 Ma (Table 1).

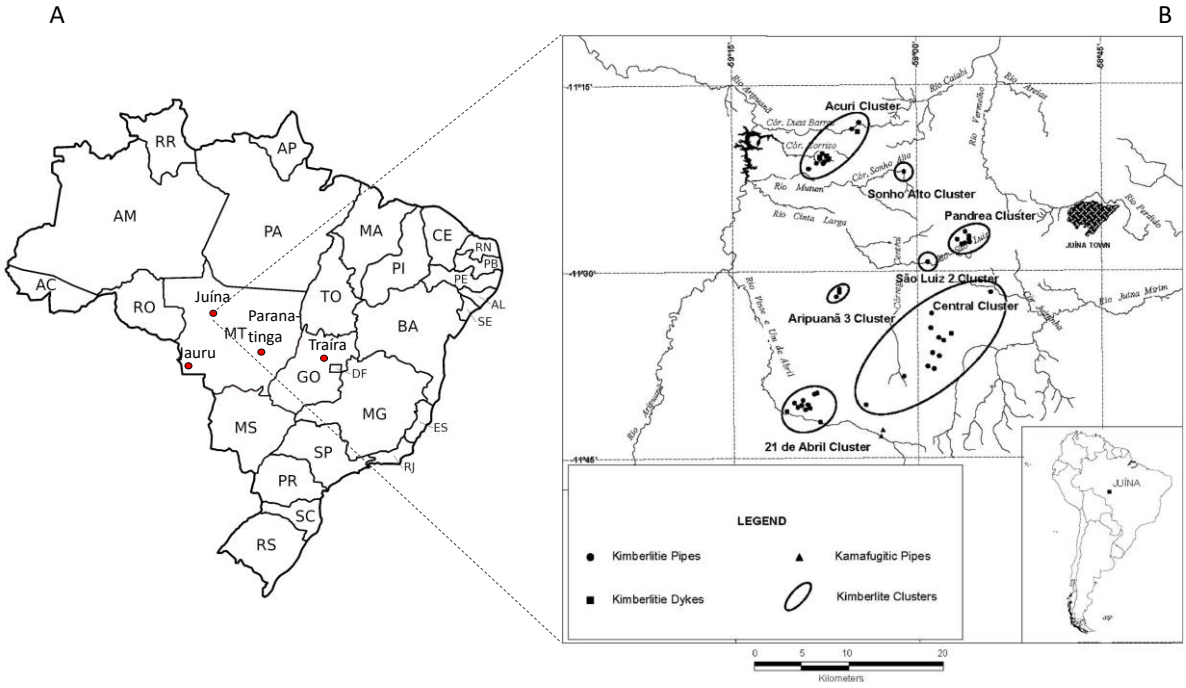

Figure 1. A. Kimberlite fields, namely Juína, Paranatinga, Traíra and Jauru (Brazil). B. Juína Kimberlite Field of Juína (adapted from Kaminsky et al., 2010).

Most of these intrusions are embedded in Permo-Carboniferous sedimentary rocks of the Parecis Basin (Fazenda da Casa Branca Formation; Siqueira, 1989), in the southern portion of the Amazon Craton (Figs. 2, 3). Other bodies of the Juína kimberlite field occur embedded in granites and gneisses of the Paleoproterozoic basement of the Rio Negro-Juruena Geochronological Province. The kimberlite intrusions are embedded in the Paleozoic sedimentary rocks of the Parecis Basin where extrusive pyroclastic deposits developed. Several intrusions in the crystalline basement (Teixeira et al., 1989). May suggest there is more post-emplacement erosion in this region and that the original pipes were eroded away lefting the kimberlite root zone

Zircon is a ubiquitous trace mineral in many igneous, metamorphic, and clastic sedimentary rocks (Patchett,et al., 1981; Kinny et al., 1991). Its ability to concentrate U and exclude Pb forms the basis of U–Pb geochronology; its refractory nature and growth patterns create robust records of crystallization ages. The ability to analyze Lu–

boletim paranaense de Geociências
ISSN: 0067-964X

Hf isotope ratios in a sample that has been dated with U–Pb methods, directly links the igneous compositions to known geological events and thus has opened many new and exciting avenues for maphic magmatic studies. (Thirlwall and Walder, 1995; Amelin et al., 1999).

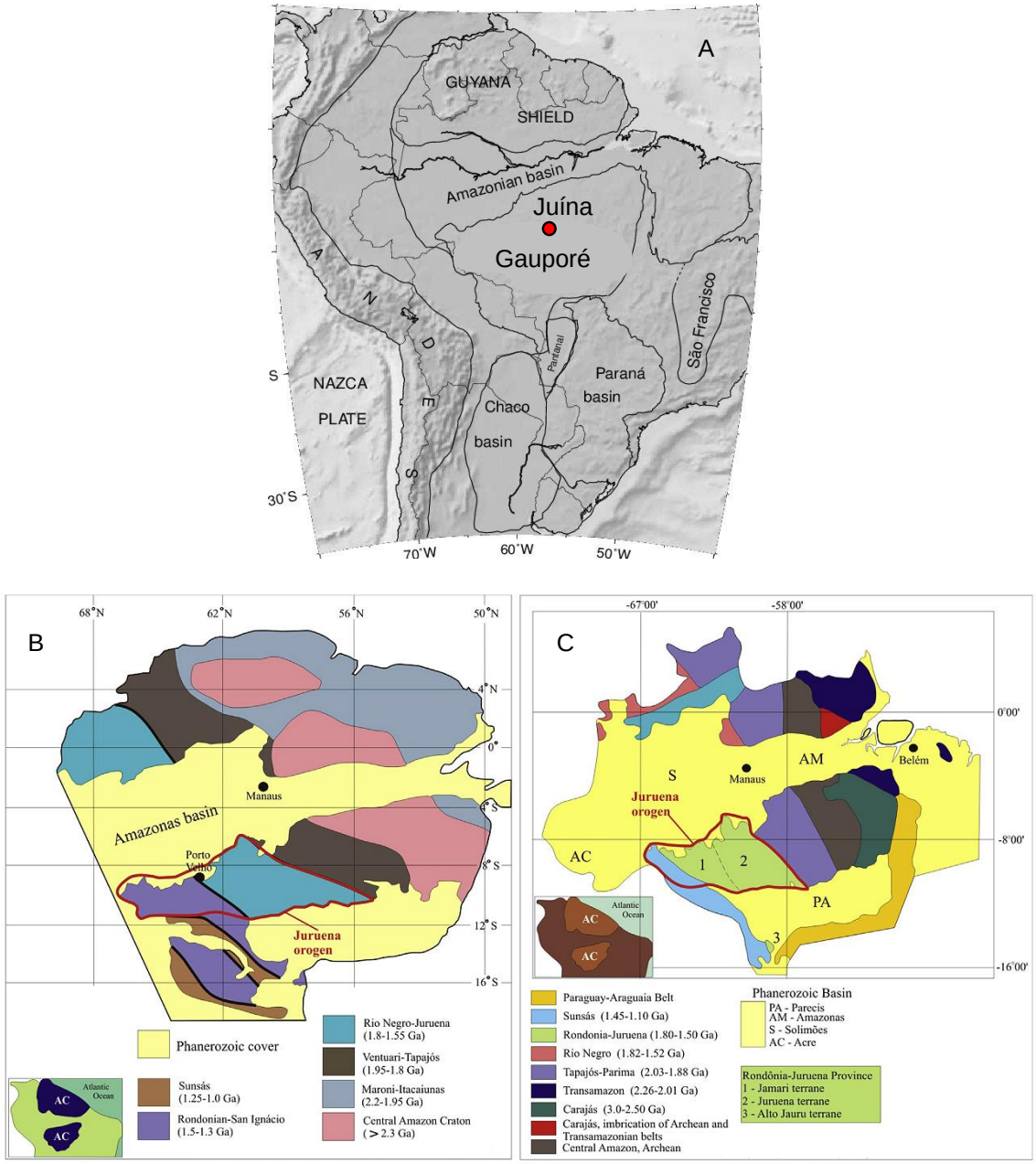

Figure 2. A. Location of the Amazonian craton (van der Lee et al., 2001), as well as; B. the main geochronologic provinces and; C. geologic provinces set (according to Scandolara et al., 2017 and references herein).

The application of Hf isotopes in zircon has been well developed in the past two decades to trace rock origin and the evolution of crust and mantle over time. In contrast, much less attention has been paid on the Hf isotope composition of zircon that grew during mantle melting events. It is usually viewed as a nuisance when studying the Hf isotope composition of original igneous rocks (Griffin et al., 2000; Amelin et al., 2000). As a result, there is comparatively little information on the Hf isotope composition of zircon grown during mantle extraction processes. This may permit in situ U–Pb dating to make a

boletim paranaense de Geociências
ISSN: 0067-964X

fundamental contribution to understanding of the mechanisms leading Hf isotope variation in zircon (Griffin et al., 2002; Andersen, et al., 2002).

In addition, a reliable determination of initial Hf isotope systematics in igneous protoliths necessitates deciphering of the structural and age complexity of metamorphic zircons (Bodet and Scharer, 2000; Kinny and Maas, 2003). This paper presents a combined intragrain study of Lu–Hf and U–Pb isotopes in zircon from kimberlitic zircon graisn in Brazil. The results provide an insight into sublitospheric mantle orogin on the zircon Lu–Hf systematics because both chronometric analyses were in situ accomplished in combination with CL imaging.

This work aims to determine the crystallization age of Juína zircon grains obtained in recent fluvial sediments using the U-Pb method by LA-MC-ICP-MS. In addition, Lu-Hf analyses were performed on the same U-Pb dated zircon grains to investigate the sources of kimberlite magmas. This work also intends to develop an analytical procedure for dating young rocks, with low uranium content, as happens with zircons from kimberlite bodies in Juína (Brazil). For this purpose, the zircon grains were analyzed in terms of textural homogeneity and U-Pb isotopic composition. Procedures for acquisition of crystallization ages by the U-Pb method were implemented, as a function of the laser ablation crater size variation and analyzed the quality of the acquired analytical results.

2. REGIONAL GEOLOGY

Juína is located in the southwestern portion of the Amazonian Craton (Fig. 2) (Almeida et al., 1981), in the Rio Negro-Juruena Province (Tassinari et al., 1996) and is constituted by Precambrian plutono-volcanic terrains, Proterozoic sedimentary basins and Juro-Cretaceous, Paleogene/Neogene platform coverage and Neogene surface formations.

2.1 The basement rocks

The most important cratonic consolidation recorded in the Amazonian Craton occurred at the beginning of the Transamazonian orogeny, at the Early Proterozoic (2.25-1.9 Ga), with the addition of the Maroni-Itacaiúnas Province (2.2-1.95 Ga) to the north and northeast of a stable Archean center (2.3 Ga) (Brito Neves et al., 1990).

From the Middle to Late Proterozoic, during the Uruaçuan Orogeny (1.9–0.9 Ga), several mobile belts, with ages between 1.78–1.0 Ga and a NW-SE structural trend, converged on each other in the northeasterly direction, on the southwestern edge of the central Archean center, to form the Amazonian Craton (Tassinari and Macambira, 1999). The continuous processes of collision and subduction produced a large volume of granitoid rocks, many of them with juvenile isotopic signatures. There is no evidence of Archean bedrock remains in the region (Cordani and Teixeira, 2007). The studied area is located in the Rio Negro-Juruena Province (1.78–1.55 Ga), which extends for approximately 900 km in length and 600 km in width in the western portion of the Amazon Craton (Martins and Abdallah, 2007).

The Geological Map (scale 1:250,000) Sheet of Juína (Melo and Franco, 1980), shows that the southern region contains the Paleo-Mesozoic sedimentary rocks of the Parecis Basin, which lie on the basement represented by the Serra da Providência Suite (Figs. 2, 3). According to the general classification of Klein et al. (1985), this basin was formed by internal fractures with vertical movements resulting from crustal distension and into an inland depression basin (Kingston et al., 1983).

boletim paranaense de Geociências
ISSN: 0067-964X

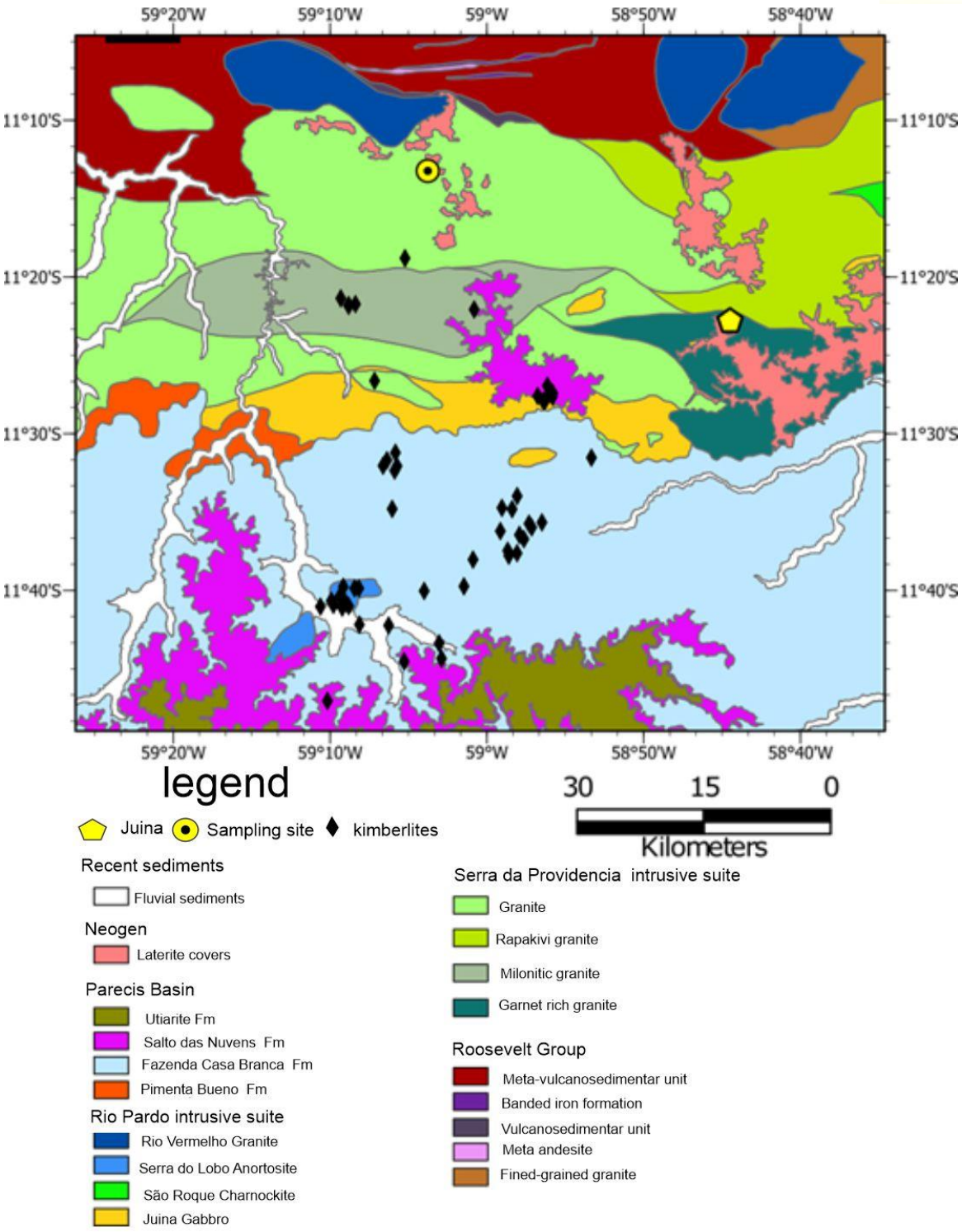

Figure 3. Regional geological map with host units of kimberlite intrusions (adapted from Melo and Franco, 1980).

The Paleozoic basin evolved through old fractures and the implantation of an intracontinental rift. These structures gave rise to the development of three sub-basins filled with sandstones and siltstones deposited from the Devonian to the Cretaceous, represented by the Pimenta Bueno, Fazenda Casa Branca and Rio Ávila formations and by the Parecis Group (Salto das Nuvens and Utiariti formations), according to Pedreira and Bahia (2004). Geological and geophysical data showed that the basin is intracratonic, deep (5,500 m), with prolonged subsidence, with a marked marine influence in the Paleozoic and provided the potential for hydrocarbons

boletim paranaense de Geociências
ISSN: 0067-964X

(Pedreira and Bahia, 2004). During the Mesozoic (Juro-Cretaceous), the Amazonian Craton was affected by another extensional event, related to the separation between South America and Africa, when depressions were filled by sedimentary and volcanic rocks from the Parecis Basin and by basaltic flows from the Tapirapuã Formation, with a Pb-Pb age of 198 Ma (Marzoli et al., 1999).

2.2 The diamondiferous Guaporé Province

The kimberlite diamondiferous province of Juína (Schultz Filho, 1981) is located in the southern part of the Amazonian Craton and its kimberlite bodies and related rocks are intrusive in the sedimentary rocks of the Parecis Basin and in the Paleo-Mesoproterozoic basement rocks. This diamond-bearing province is called Gauporé (Fig. 2). These intrusions are generally limited by N55ºW lineaments that cut the northern edge of the Parecis Basin and include the Juína kimberlite group, with an intrusion age from the Lower Jurassic to the Upper Cretaceous (Nannini et al., 2017).

U/Pb dating, in zircon from Juina kimberlites, performed by Teixeira (1996), revealed ages ranging from 95 to 92 Ma (Table 1). The area also has secondary deposits such as alluviums and Paleogene/Neogene lateritic covers and Neogene deposits of sand, clay, and gravel, sometimes diamondiferous, deposited along the main watercourses (Melo and Franco, 1980).

About forty-five diatremes were recognized in the kimberlite province of Juína (Fig. 1), which form large circular craters, with up to 55 ha, mainly composed of subaerial pyroclastic rocks, hydroclastic tephra and volcaniclastic deposits (Teixeira et al. 1998). U-Pb isotopic studies (Table 1) in zircon grains recovered from Juína and Paranatinga kimberlites indicated two distinct periods for the formation of these zircon grains: a Cenomanian (91.6 - 94.6 Ma) for Juína and another Barremian (122.6 - 126.3 Ma) for Paranatinga (Heaman et al., 1998).

The main forms of relief in the region are described as Parecis Plateau, the Southern Amazon inter-plateau depression and the Residual Plateaus of Northern Mato Grosso. The Parecis Plateau occurs in the southern portion of the area and was carved out of sedimentary rocks from the Parecis Basin. The secondary diamond deposits are found in interfluvial areas represented by the main rivers in the region (Fig. 1), with the highest elevations between 380 and 450 m. The relief of this region is composed of plateaus, partially lateralized, evidence of a regional leveling surface, known locally as “chapada”. The drainage of this unit has a preferential rectangular pattern (Nannini et al., 2017).

The Southern Amazon inter-plateau depression is a large area, and its name derives from the lowered and confined area between the mountains and plateaus of Cachimbo, to the north, and the Planalto dos Parecis and/or Chapada de Dardanelos, to the south. According to the Geological Sheet of Juína, published by CPRM (Melo and Franco, 1980), this inter-plateau zone extends throughout the central-northern portion of the Mato Grosso state, with altitudes from 200 to 420 m, where it is delineated relief of convex shapes, carved mainly on granitic rocks of the Providência Suite Mountain and, to a lesser extent, on volcano-sedimentary rocks. Drainage from this unit has a dendritic pattern. The depression is marked by accentuated relief dissection, with 500 m high plateaus, especially in the transition strip to the Parecis Plateau. Between the depression and the plateau, the lower elevations give way to the higher reliefs through successive erosion surfaces. The Residual Plateaus of northern Mato Grosso occur in the northwestern part of the Geological Sheet of Juína (Melo and Franco, 1980), in volcano-sedimentary terrains, and are characterized by convex top relief and tabular forms with different dimensions, reaching locally an elevation around 400 m (Martins and Abdallah, 2007).

The clusters of kimberlite bodies in the Juína region are defined by the mined areas for secondary deposits, formed by river sediments (Silveira, 2016). Costa (2013)

boletim paranaense de Geociências
ISSN: 0067-964X

observed mantle xenoliths in Juína kimberlites composed mainly of peridotites. The kimberlite mineralogy reported (Nannini et al., 2017) is composed of clinopyroxene, garnet, orthopyroxene, spinel, zircon and diamond. Pyroxene grains exhibit equigranular textures and intense silicification, replacing olivine and orthopyroxene by cryptocrystalline quartz.

The studies reported by Kaminsky et al. (2010) suggest that the kimberlitic intrusion in the Juína region presents super-deep diamonds that originated in the lower mantle (Harte et al., 1999; Kaminsky et al., 2001a, 2009) with depths of up to 660 km. According to these authors, the existence of mineral inclusions in Juína diamonds, such as a higher iron content in ilmenite, chromium spinel and olivine may reflect a core/mantle convection process interpreted by Walter et al., (2008) as a super-deep subduction and partial melting of the lower mantle and subsequent rise of kimberlite magma.

Wirth et al. (2007) reported the identification of a nanocrystalline hydrated aluminum silicate (AlSiO3-OH) phase in association with stishovite found in one of the Juína diamonds. This phase is stable at pressures up to at least 1625 °C and 17 GPa (Sano et al., 2004), and may indicate that Al-rich sediments or hydrated basalts were subducted to the transition zone depth. Within other Juína diamonds, several syngenetic 20-50 µm sized carbonate inclusions have been found in situ in association with Ca-walstromite and 'olivine' (Brenker et al., 2007). The origin of these lower mantle carbonates is likely related to lithospheric material transported to great depths via subduction processes (Kaminsky et al., 2010).

Table 1 - Dates obtained on Juína Kimberlite zircon grains in the literature.

U-Pb Age (Ma)	References
79.2 to 80.1	Davis et al., 1977
92 to 95	Teixeira et al., 1996
91.6 to 94.6	Heaman et al., 1998
93.7±0.7 Ma	Kaminsky et al., 2010
93.4±0.8 Ma	Kaminsky et al., 2010
92.9±1.0	Kaminsky et al., 2010
93.5±0.7	Kaminsky et al., 2010
93.7±0.7	Kaminsky et al., 2010
93.7±0.7 Ma	Kaminsky et al., 2010

3. MATERIALS AND METHODS

Samples of zircon grains were obtained in Juína area, where zircon appears in the tailings of gravimetric concentration plants. From a group of 70 zircon grains, 14 grains were selected to avoid inclusions (Fig. 4A) and organized in “mounts” containing five grains and whose preparation is described below. The mounts were designated with letters A to E and included the following zircons: mount A with grains ZRJ-1 to ZRJ-5; mount B with grains ZRJ-6 to ZRJ-10; mount C with grains ZRJ-11 to ZRJ-15; mount D with grains ZRJ-16 to ZRJ-20 and; mount E with grains ZRJ-21 to ZRJ-24.

boletim paranaense de Geociências
ISSN: 0067-964X

The zircon samples were fixed in epoxy resin (Fig. 4B and C) in a circular mold with an internal diameter of 4 cm. The mold containing the materials to be analyzed was filled with epoxy resin heated in an oven for 24 hours at 40ºC. The mount face containing the zircon grains was polished after hardening. Aluminum oxide sandpapers with grain sizes ranging from 127 to 15.3 µm were used, in a sequence of abrasives of progressively smaller granulometry until reach half of the grains, thus allowing the visualization of the inner part of the grain. After this procedure, diamond pastes with grain sizes ranging from 3 to 0.25 µm were used, until the resin and the grains to be analyzed be polished enough for imaging by scanning electron microscope (SEM).

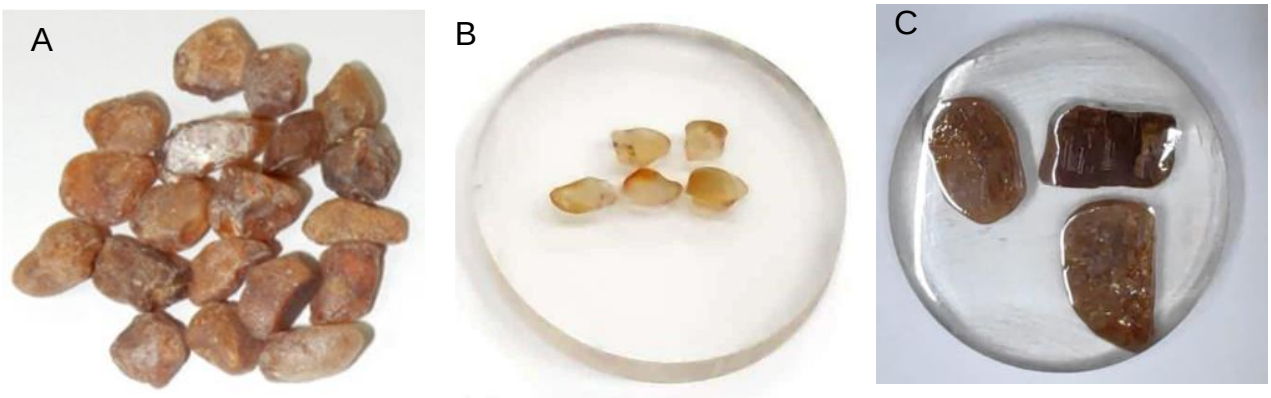

Figure 4. A. Zircon grains from the Juína kimberlite province; B. mount G with 5 zircon fragments; (C) Mount A with 3 zircon grains.

3.1. U-Pb geochronological method

The U-Pb zircon method is a radiometric dating technique for minerals aiming to establish the age of crystallization and/or metamorphism, based on the decay systems of the U and Th isotopes for stable Pb isotopes. These decay systems are fundamental in geological studies, since the half-life of natural Uranium radionuclides is long, enough to cover the entire history of the Earth, and short enough so that radioactive and radiogenic isotopes can be quantified in uranium-concentrating minerals (Davis et al., 2003).

The Pb element has four naturally occurring stable isotopes, ^{204}Pb, ^{206}Pb, ^{207}Pb and ^{208}Pb, of which the last three have a radiogenic component produced by the independent decay of ^{238}U, ^{235}U and ^{232}Th, respectively. The U-Th-Pb geochronology can be explained by the decay of several parent isotopes to different stable Pb isotopes, each one with specific half-life. The parent isotopes follow a sequence of alpha and beta decays (which implies the ejection of an alpha or beta particle, respectively, from the nuclei), generating a series of intermediate daughter isotopes, and always leading to the same stable isotope of Pb (Bateman, 1910).

In a closed system, all decay chains will reach secular equilibrium in a time proportional to the longer half-life of the intermediate daughter isotope. The system will remain in equilibrium until one or more isotopes in the chain are fractionated from others, either by chemical partitioning in a magmatic system, low temperature fractionation or chemical weathering. In secular equilibrium, one ^{206}Pb atom is created for every ^{238}U atom that decays, but if this equilibrium is disturbed during crystallization or partial melting, the calculated apparent age is compromised.

One of the main forms of data visualization is the concordia diagram that was introduced by Wetherill (1956), which plots the ^{206}Pb/^{238}U vs. the ^{207}Pb/^{235}U ratio of the same analysis. The concordia parametric curve can be drawn for equal values of time (t), where the

boletim paranaense de Geociências
ISSN: 0067-964X

contribution of the initial Pb is considered insignificant compared to the radiogenic component. Samples that remained with the closed system since its formation plot on the concordia curve, while those that had their system open, are distant from the curve, being called discordant. As the half-life of ^{238}U (4.5 x 10^9 years) and ^{235}U (7.04 x 10^8 years) are different, this relationship is not linear. Discordant arrangements are generally caused by Pb and U loss and gain and mixing of materials with different ages (Williams et al., 1984).

In the acquisition of data to determine the U-Pb and Lu-Hf ages, the GJ-1, 91500 and Mud Tank zircon standards were used as reference materials, and the following sequence: blank, GJ-1 standard, Mud Tank, 10 ablation craters of the analyzed grain, pattern GJ-1, pattern 91500 and blank again. It is understood as blank, the analysis without material ablation, taking into account the elements present at that moment in the carrier gas and the electronic variations of the equipment. The equipment used in the isotopic analysis was a Thermo Finningan NEPTUNE PLUS MC-ICP-MS coupled with a Laser Ablation Photon Machine ANALYTE G2 system with a 193nm laser located at the Multiuser Laboratory for Environment and Materials - MultiLab/UERJ. The configuration of Faraday and compact discrete dynode (CDD) collectors for U-Pb isotopic analysis are presented in Table 2. Afterwards, a battery of analyzes were carried out in order to obtain the most reliable age, which was achieved using craters with an ablation diameter of 150 µm. The concordia diagrams for age determination by the U-Pb method were produced with the Isoplot software (Ludwig, 2004).

3.2. Lu-Hf geochronological method

^{176}Lu is an unstable radionuclide that spontaneously decay by beta (β) emission to stable ^{176}Hf, with a half-life of approximately 37 Ga (Scherer et al., 2001). ^{176}Lu also decays to ^{176}Yb, by electron capture, but in an amount that can be disregarded for age calculations (Geraldes, 2010). Variations in the abundance of ^{176}Hf are conventionally expressed in relation to ^{177}Hf, whose natural abundance is constant.

The Lu-Hf method is a powerful tool to decipher the crustal and mantle evolution of the Earth, due to the high concentration of Hf in zircon, contrasting with very low Lu-Hf ratios (Hawkesworth and Kemp, 2006). The Lu-Hf isotopic system can be used to trace the history of the Earth's chemical differentiation (crust and mantle) since Lu and Hf fractionation occurs concurrently with magma generation (Patchett et al., 1981). The initial Lu/Hf ratio of Earth's chondrite has been progressively modified, over time, through episodes of partial fusion of the upper mantle. The generation of basaltic magmas depleted the residual mantle in Hf (the most incompatible of these two elements) enriching the basalt crust thus generated. Over time, the Hf isotopic composition of the depleted mantle (Lu/Hf > chondrites) and enriched crust (Lu/Hf < chondrites) diverges from any remaining unfractionated material (Lu/Hf = chondrites).

Thus, samples with $^{176}Hf/^{177}Hf$ ratio greater than that of the chondrite, at a time, t, have positive εHf values, while those with a $^{176}Hf/^{177}Hf$ ratio lower than that of CHUR have negative εHf. Chondrites have εHf equal to zero (Kinny and Maas, 2003). Positive values of εHf imply that the Hf originated from an impoverished source, with a Lu/Hf ratio greater than that of the chondritic reservoir (εHf >0) indicates that the magma was extracted from the depleted mantle. On the other hand, the negative values imply an enriched source derivation, with a low Lu/Hf ratio in relation to the chondritic reservoir, consequently, εHf <0 is typical of rocks formed by the fusion of old crust.

It is possible to calculate a model age (TDM), in relation to the depleted mantle. This age is related to the time elapsed since the generation of the sample from a magma with a $^{176}Hf/^{177}Hf$ ratio similar to the depleted mantle. Whereas a single TDM age stage is commonly calculated for whole rock analyses, for zircon studies two TDM age stages are

boletim paranaense de Geociências
ISSN: 0067-964X

required (Nebel et al., 2007). The TDM age in zircon is calculated from the initial Hf isotopic composition of the zircon, using the average of the crustal Lu/Hf ratio. The initial Hf composition represents the $^{176}Hf/^{177}Hf$ value calculated at the moment when the zircon crystallized, that is, it is equivalent to the U-Pb age previously obtained in the same crystal. These model ages indicate the crustal residence time for the rocks that hosted the zircon. Thus, the importance of performing U-Pb and Lu-Hf measurements on the same portion of the zircon grain is evident, so that the εHf and TDM values can be recalculated at the moment of its crystallization.

Concordia diagrams (Watheril, 1956) were performed for each grain and for all grains aiming to identify procedures that improve the quality of the results.

The equipment used in the isotopic analysis was a Thermo Finningan NEPTUNE PLUS MC-ICP-MS coupled with a 193nm laser Photon Machine ANALYTE G2 Laser Ablation system belonging to the Multiuser Laboratory for Environment and Materials - MultiLab/UERJ. The acquisition of Lu-Hf data is carried out following a sequence that begins with the choice of the grain to be analyzed and the place where the crater will be made, usually in the place where the U-Pb age was performed, however with a diameter of 40-50µ. For this, the CL images and the image provided by the equipment's camera are counted on, then the laser spot is positioned, and the beam is manually activated, initiating the ablation process. Material ablated by laser was carried using Ar and He and it takes a few seconds (3-10) for the signal to stabilize. In sequence, data acquisition is initiated in 40 cycles (1.045 seconds each cycle).

The collectors were positioned as follows (Table 3): in the central collector the mass ^{176}Hf, in the collectors H1 mass ^{177}Hf, H2 mass ^{178}Hf and H3 mass ^{179}Hf. In the collectors L1 the mass ^{175}Lu, L2 the mass ^{174}Hf, L3 the mass ^{173}Yb and in L4 the mass ^{171}Yb. The isobaric corrections were installed in the mass spectrometer software, so that the interferences ^{176}Lu and ^{176}Yb have their abundances obtained through the measurements of the masses ^{173}Yb and ^{175}Lu. Thus, the correction factors of 0.795015 and 0.026580, respectively, were used. The correction of the isotopic fractionation of the mass spectrometer is performed from the constant ratios ^{179}Hf / ^{177}Hf (true value 0.7325) and ^{171}Yb / ^{173}Yb (true value of 1.123456) reported in the literature (Patchett and Tatsumoto, 1980, 1981; Morel et al., 2008).

The values of the abundances of the Hf, Lu and Yb isotopes were shown to be effective according to three reference material used (GJ-1, Mud Tank and 91500). In the calibration of the Lu-Hf method using laser ablation, the $^{176}Hf/^{177}Hf$ ratios of the GJ-1 reference material were initially analyzed. The GJ-1 (Fig. 1) is used in large scale by geochronology laboratories being reference material for U-Pb and Lu-Hf isotopic analysis. The isotopic ratios $^{176}Lu/^{177}Hf$ and $^{176}Hf/^{177}Hf$ of this reference material are reported in the literature (Woodhead et al., 1995; Elhlou et al. 2006; Moreal et al. 2008) with values of 0.00025 and 0.282005 ± 5, respectively. In the calibration of the method using laser, the $^{176}Hf/^{177}Hf$ ratios of the GJ-1 similar to the reference material published were obtained. Its mean value is 0.282016 ± 5, which is almost identical to the recommended value in the literature.

A second reference material used during the analysis is comprised of the Mud Tank (Fig. 1), a natural zircon collected a carbonatite that outcrops in Strangways, east of Alice Springs (Australia). The carbonatite has an age of 732 Ma with large amounts of zircon and apatite crystals up to ten centimeters. The obtained isotopic ratios $^{176}Lu/^{177}Hf$ and $^{176}Hf/^{177}Hf$ indicate values of 0.000042 ± 6 and 0.2882507 ± 6 and are equivalent to those described in the literature for the Mud Tank reference material (Woodhead et al., 1995). The 91500 (Fig. 1) reference material is also used and was part of the Harvard museum collection and was carefully prepared as a reference material after a preliminary characterization, including Lu-Hf isotopic analyzes. Zircon 91500 has been widely adopted by many laboratories as reference material for Lu-Hf analyzes. The

boletim paranaense de Geociências
ISSN: 0067-964X

isotopic ratios values of 0.000311 ± 8 ($^{176}Lu/^{177}Hf$) and 0.2882305 ± 8 ($^{176}Hf/^{177}Hf$) were determined and are consistent with the reported true value (Elhlou et al., 2006; Morel et al., 2008).

3.3. Imaging of zircon grains

The fourteen centimetric zircon grains were mounted in resin and polished to perform images by cathodoluminescence aiming to assess the internal structure of the zircon. The techniques used for imaging the samples were cathodoluminescence (CD) by optical microscopy and electron microscopy (SEM). In the case of optical microscopy, the image contrast is the result of the difference in light reflectivity in the different regions of the microstructure, since the system is basically constituted by the source of the electron beam coupled to an optical microscope with a digital camera for image records. For opaque materials illuminated with visible light only the surface can be seen and it needs to be carefully prepared in order to reveal the details of microstructure.

The internal structure of the zircon such as inherited cores, resorption areas, magmatic zoning among other features, can be revealed through images produced by SEM-Cathodoluminescence (SEM-CL). In this investigation were used the cathodoluminescence CITL Mk5-2 coupled to the LEICA DM4500 P Microscope and the Scanning Electronic Microscope – MEV FEI Quanta 250, respectively. In addition, 20 kV voltage and spot size 6.0 were used for obtaining images.

For electronic imaging of minerals such as zircon, as they are not conductors, the grains must be metallized. Metallization consists of coating the surface of the sample to be imaged with a layer of conductive material. In this case, metallization with gold was applied. The images allowed to characterize features such as fractures and inclusions and growth phases and to select the area to produce the crater for sample volatilization in the LA-MC-ICP-MS procedure.

4. RESULTS AND DISCUSSION

4.1 Results of U-Pb analysis for the mounts A and B (zircon grains ZRJ-1 to ZRJ-10)

The results of U-Pb analyses for the mounts A and B, designated as zircon grains ZRJ-1 to ZRJ-10 are presented in (Appendix 1). Images using optical cathodoluminescence (optical-CL) for zircon grains ZRJ-1 to ZRJ-5 and the craters where laser shots were taken during isotopic analyses are shown in Fig. 5. The concordia diagrams for age determination by the U-Pb method for those zircon grains (ZRJ-1 to ZRJ-10) provided the following ages determined with a 110 µm ablation crater: ZRJ-1: 98.8 ± 6.2 Ma, with MSWD=0.24 (Fig. 6A); ZRJ-2: 89 ± 10 Ma, with the statistical index Mean Square of Weighted Deviated (MSWD) =0.34 (Fig. 6B); ZRJ-3: 85.7±4.9 Ma, with MSWD=0.36 (Fig. 6C); ZRJ-4: 91 ± 21 Ma, with MSWD=0.072 (Fig. 6D) and; ZRJ-5: 87.4 ± 4.7 Ma, with MSWD=0.095 (Fig. 6E). Data from these 5 (ZRJ-1 to ZRJ-5) grains gathered in a concordia diagram generated a joint age (ZRJ-1 to ZRJ-5) of 89.3 ± 2.2 Ma, with MSWD=0.52 (Fig. 6E).

Images using optical cathodoluminescence (optical-CL) for the fragments of sample B, here designated as ZRJ-6 to ZRJ-10 and the craters where laser shots were taken during isotopic analyses are shown in Fig. 7. For those zircon grains were estimated the following ages using a 110 µm ablation crater: ZRJ-6: 94.4 ± 8.7 Ma, with MSWD=0.12 (Fig. 8A); ZR-7: 89±12 Ma, with MSWD=0.037 (Fig. 8B); ZRJ-8: 99.2 ± 8.0 Ma, with MSWD=0.13 (Fig. 8C); ZRJ-9: 91.8 ± 1.5 Ma, with MSWD=0.28 (Fig. 8I); ZRJ-10: 85.5 ± 4.3 Ma, with MSWD=0.017 (Fig. 8J). The combined treatment of this set of grains (ZRJ-6 to ZRJ-10) provided an age of 95.8 ± 3.7 Ma, with MSWD=0.46 (Fig. 8K).

boletim paranaense de Geociências
ISSN: 0067-964X

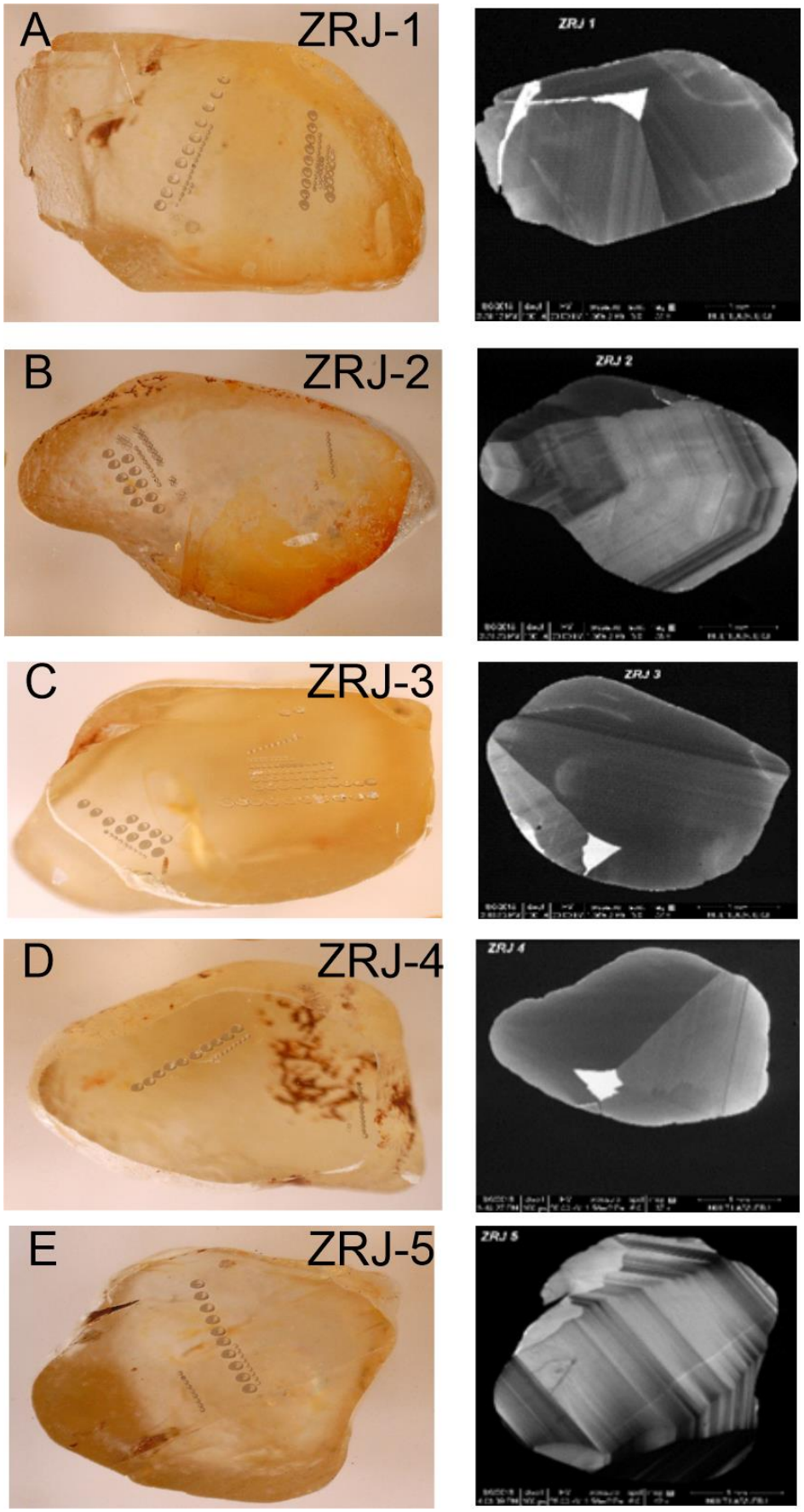

Figure 5. Imaging of the zircon grains ZRJ 1 - ZRJ 5 analyzed in this investigation using optical cathodoluminescence. The craters (with 110 µm) represent the locations where laser shots were taken during isotopic analyses.

boletim paranaense de Geociências
ISSN: 0067-964X

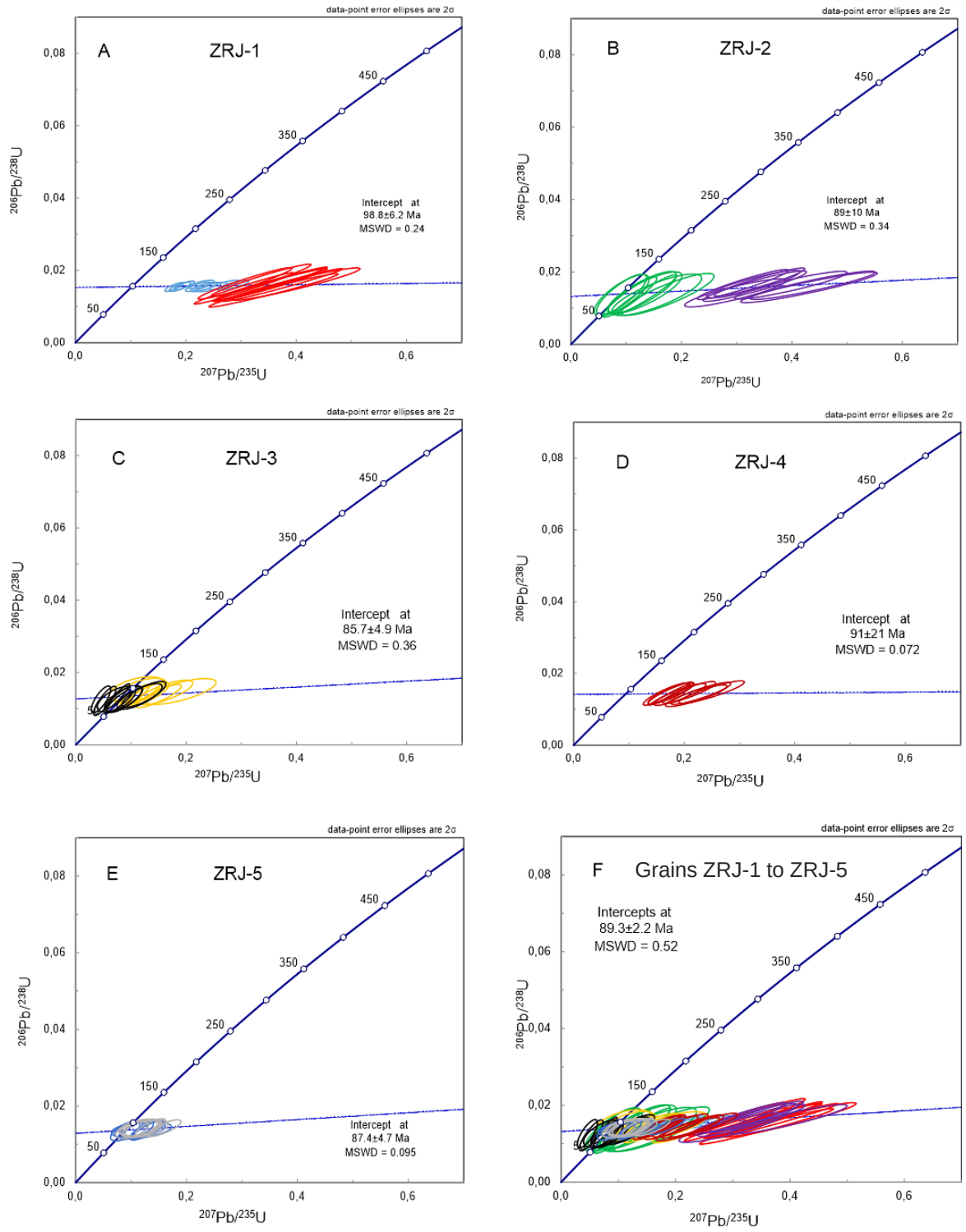

Figure 6. Concordia diagram for the grains ZRJ-1 to ZRJ-5 based on 110 µm ablation craters.

boletim paranaense de Geociências
ISSN: 0067-964X

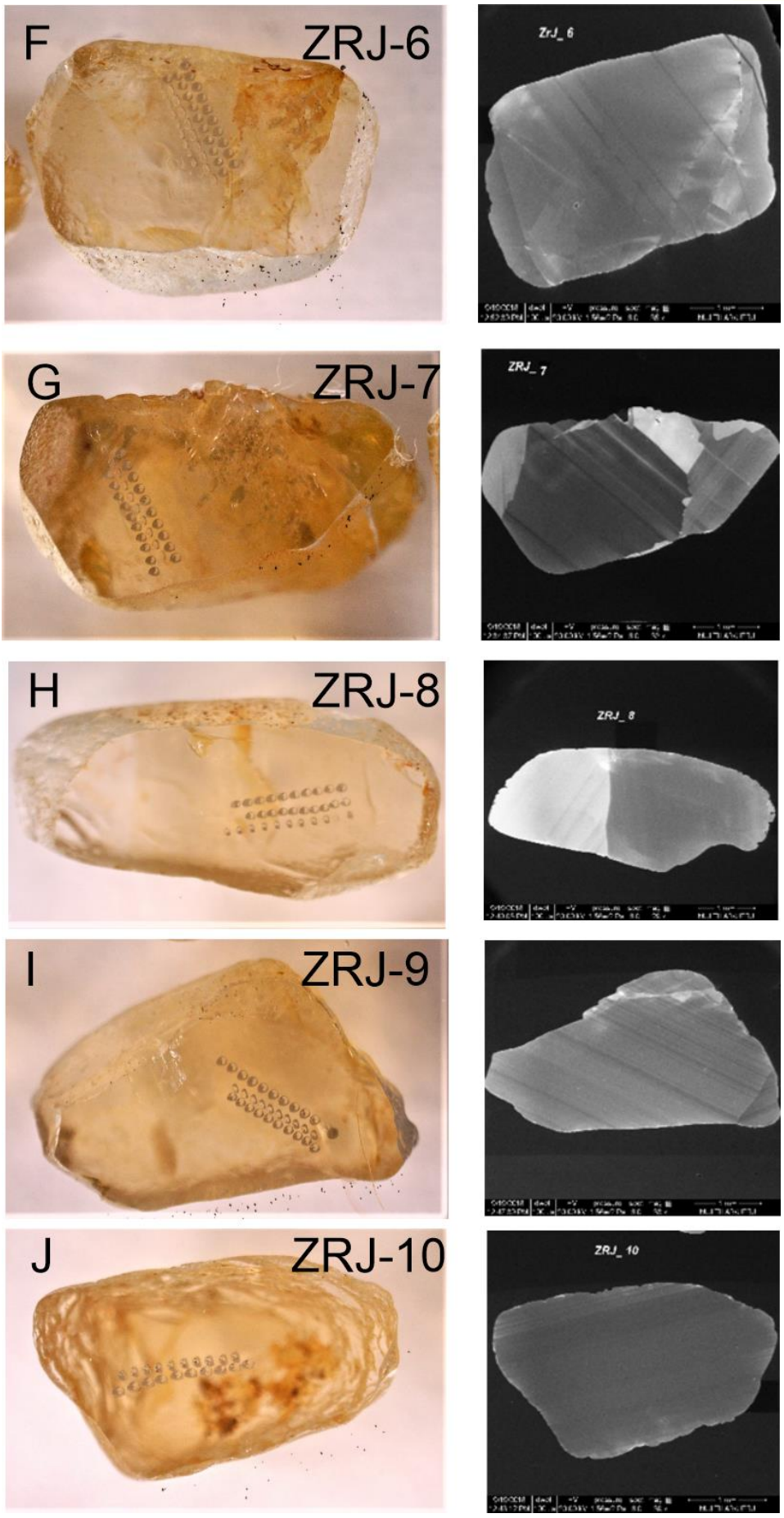

Figure 7. Imaging of the zircon grains ZRJ 6 - ZRJ 10 analyzed in this investigation using optical cathodoluminescence. The craters (with 110 µm) represent the locations where laser shots were taken during isotopic analyses.

boletim paranaense de Geociências
ISSN: 0067-964X

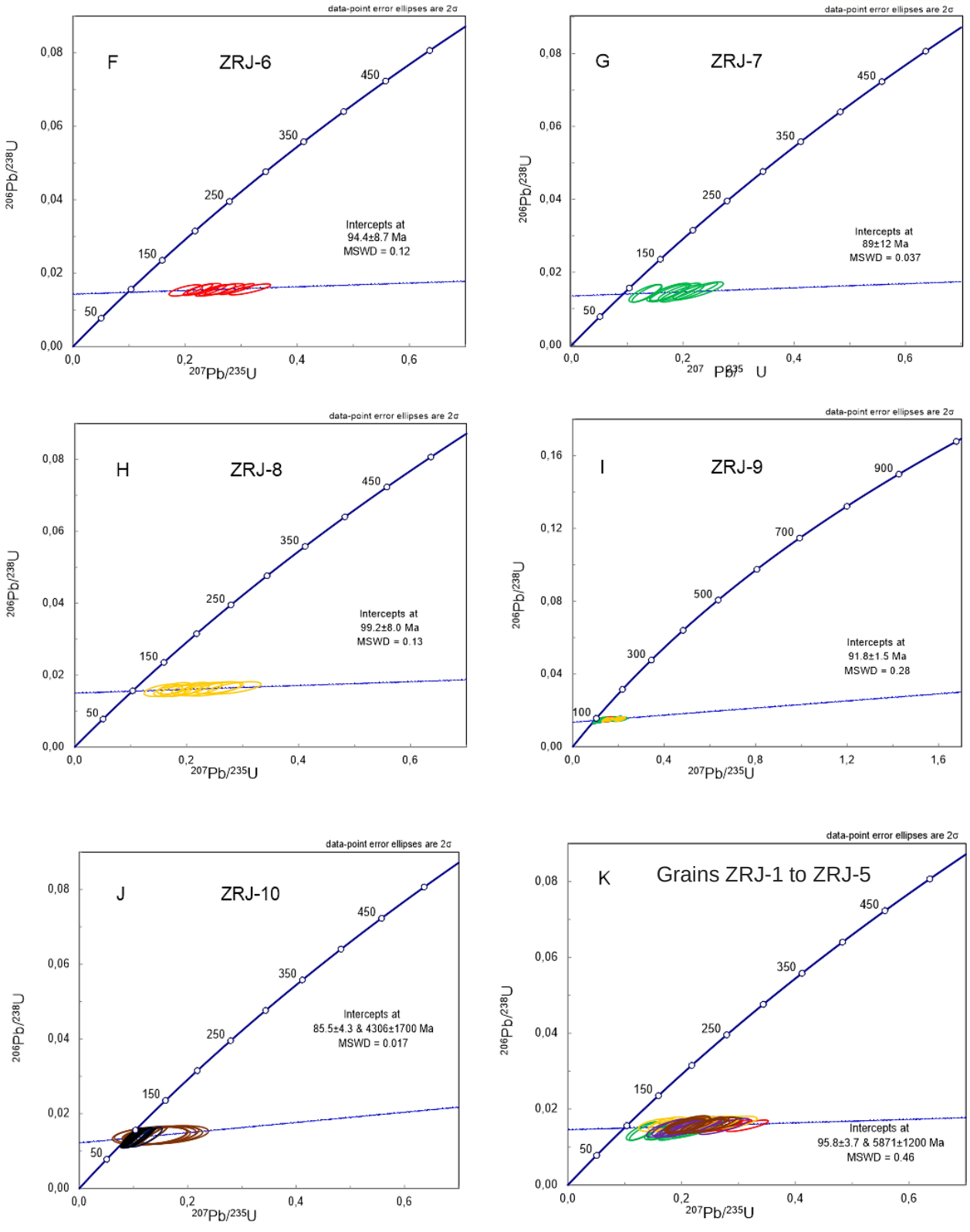

Figure 8. Concordia diagram for the zircon grains ZRJ-6 to ZRJ-10 based on 110 µm ablation craters.

boletim paranaense de Geociências
ISSN: 0067-964X

The results show that the error of the ages determined with a 110 µm ablation craters in sample B (ZRJ-6 to ZRJ-10) varied between 18.18 and 8.06%. A considerable inclination of the ellipses in relation to the axis was observed in the case of the $^{207}Pb/^{235}U$ ratios; the fragments of sample B (ZRJ-6 to ZRJ-10), do not plot on the concordia curve, as shown in Fig. 6. The ^{207}Pb analyzed in counts per second (cps) in the fragments of sample B (ZRJ-6 to ZRJ-10) provided values between 2600 and 2900 cps, on average, which demonstrates a reduced amount of this isotope compared to the realized blank that varied between 1900 and 2200 cps. Thus, it was found that the graphs of the ratio $^{206}Pb/^{238}U$ versus $^{207}Pb/^{235}U$ show that the concordia have a very elongated elliptical shape and are almost parallel in relation to the axis of the ratio $^{207}Pb/^{235}U$; this type of results are due to the fact that the rock has a young age; on the other hand, ^{235}U has a half-life shorter than ^{238}U, which results in low abundances of ^{207}Pb and a larger error in the $^{207}Pb/^{235}U$ axis.

4.2 U-Pb results for the mount C (zircon grains ZRJ-11 to ZRJ-14)

Most of the zircons observed in zircon grains ZRJ-11 to ZRJ-14 have a preserved prismatic habit, but with a certain rounding on the edges of the crystals. Catodoluminescense images show nuclei growth with oscillatory zonation, characterized by alternating light and dark bands (Fig. 9). The binocular lupe images show zircon 4-30 mm in size grains, sub-rounded, without any crystal face, appear yellowish and reddish-brown. They show brownish, yellowish and (rarely) pinkish cathodoluminescence with a predominance of yellowish hues (optical-CL). Most of the investigated crystals are homogeneous.

The zircon grains ZRJ-11 to ZRJ-14 were analyzed by the U-Pb and Lu-Hf methods. Concordia diagrams shown in Fig. 10 A, B and C were performed at the LA-MC-ICP-MS and provided the ages 84 ± 15 Ma, 89 ± 07 Ma, 88 ± 19 Ma, 88 ± 19 Ma and 99 ± 06 Ma, respectively.

4.3 Lu-Hf isotope results from the mounts A, B, C, D, E and G

The results of 200 spots analysis with εHf isotope values and Hf model ages estimated by the Lu-Hf method, in the zircon from the mounts A, B, C, D, E and G (consisting of 5 fragments of a zircon) are presented in Appendix 2. These results show that the εHf values, ranging from -15 and +8, are between the values for a chondritic reservoir (CHUR) and the zircons crystallized from magmas with depleted mantle source (Kaminsky et al., 2010).

The Hf isotopic composition of Juína zircons corresponds to the zircon average kimberlite trend (Griffin et al., 2000). The results presented show consistency with the literature data, indicating, however, little homogeneity in the analyzed samples. The εHf values of between -15 and +8 can indicate intensities of contamination of the host rocks during the intrusion of the kimberlite magma. Kimberlites and zircon megacrysts may have some relation but are generally treated separately (Nowell et al. 2004).

Since there are no Hf studies reporting Hf isotopic results in zircon graisn from kimberlites in Amazonia, the results here reported may be compared with the results reported by Costa (2013). The author obtained Sm/Nd results with negative εNd values (-8.35 to -11.31) and TDM model age from 1842 to 1114 Ma. Mineral chemistry in clinopyroxenes (from xenoliths) has the highest Al contents and low CaO content, in addition to high content of incompatible elements (up to 2,313 times than the primitive mantle) and enrichment in light rare earth elements (LREEs) in CPX, with La/Ybn =1. The magma should have a temperature between 1264°C and 1308°C. Costa and Gaspar (2001) reported nodules with graphic ilmenite-clinopyroxene intergrowth, with formation temperature of about 1264 to 130 ºC, for an estimated pressure of 45 kbar.

boletim paranaense de Geociências
ISSN: 0067-964X

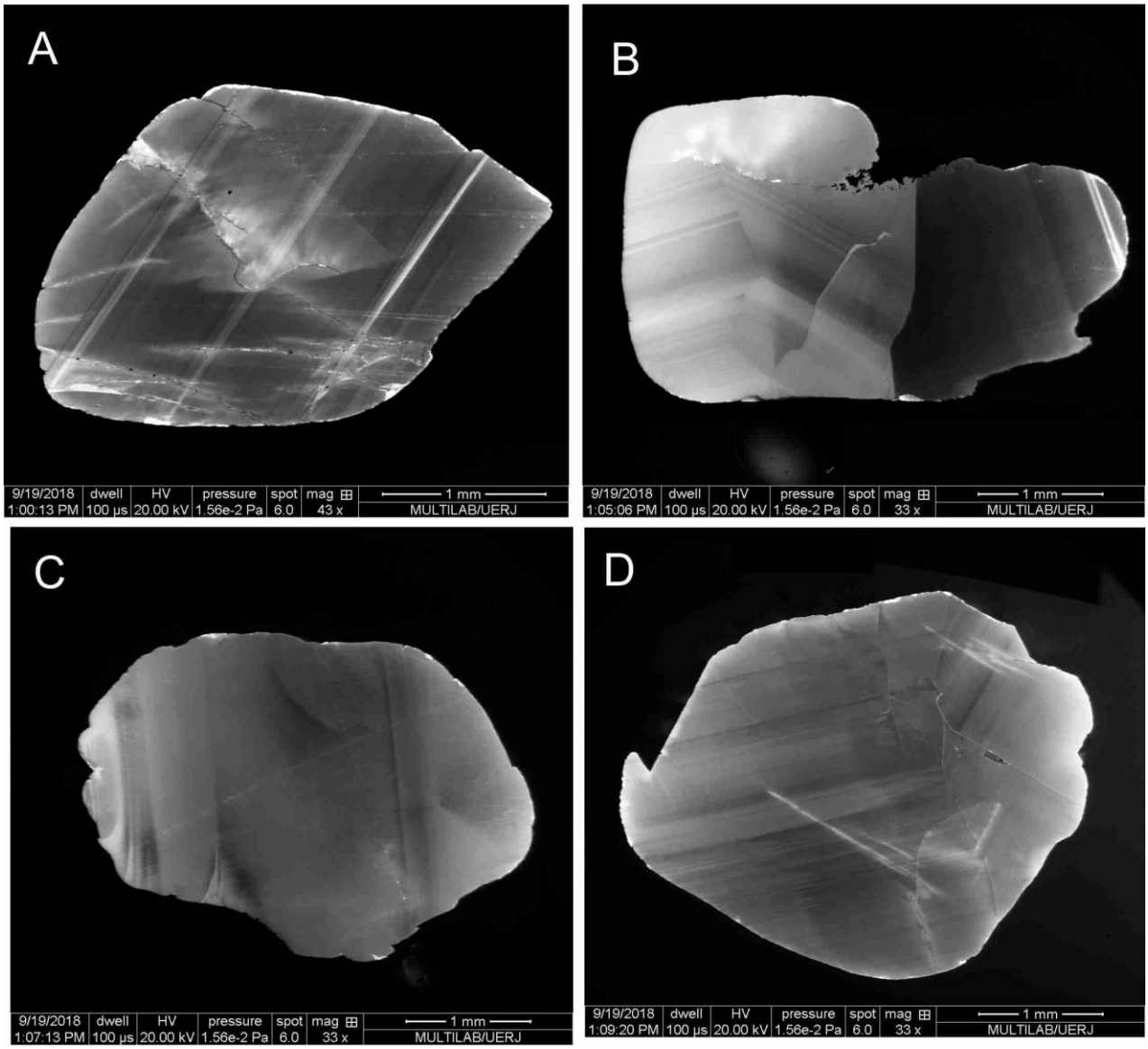

Figure 9. Cathodoluminescence images for grains (A) ZRJ-11, (B) ZRJ-12, (C) ZRJ-13 and (D) ZRJ-14

boletim paranaense de Geociências
ISSN: 0067-964X

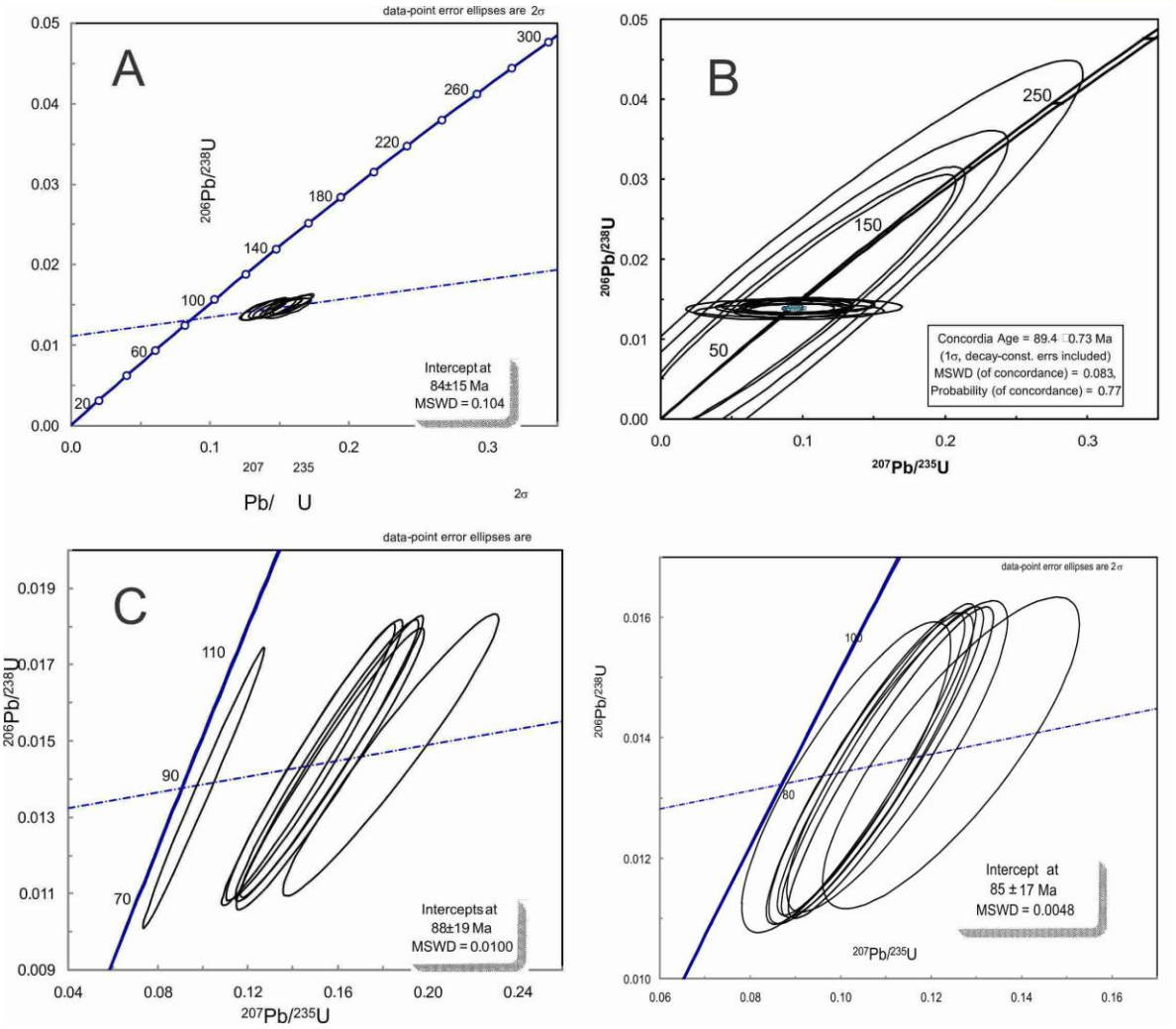

Figure 10. Concordia diagram obtained by the LA-MC-ICP-MS technique for grains ZRJ-11 (A), ZRJ-12 (B), ZRJ-13 (C) and ZRJ-14.

4.4 About the age of the Juína kimberlite intrusion and

The U-Pb ages here reported may be interpreted in the context of the Mato Grosso kimberlite fields, namely Juína, Paranatinga, Traíra and Jauru (Brazil). The ages obtained by LA-MC-ICP-MS from the concordia diagram, summarized in Table 4, ranged between 99.2 ± 8 Ma and 84 ± 15 Ma. These ages can be interpreted as composed of two distinct groups: the first between 84 and 89 Ma and the second between 91 and 99 Ma. The age of 91.8 ± 1.6 Ma, with MSWD = 0.32, was the most reliable for the Juína zircon. It was obtained using ablation craters of diameter between 110 and 150 µm. Diameters of these dimensions allow for more reliable results, using the LA-MC-ICP-MS.

The cathodoluminescence images taken in the fourteen centimetric zircon grains show that most of the investigated crystals have a non-metamict structure. Instead, these images evidence the rare presence of fractures, inclusions or overgrowth that only confer a small degree of heterogeneity to the analyzed zircon grains. They also show that those grains present a considerable degree of internal homogeneity, not showing a significant internal zoning. These characteristics suggest that the analyzed zircon grains had stable growth conditions and that their isotopic system has not been disturbed since their crystallization.The analyzed Juína zircon grains showed total concentrations of U and Th from 108-673 mg kg^{-1} and 26-194 mg kg^{-1}, respectively, and concentrations of non-radiogenic Pb varied

boletim paranaense de Geociências
ISSN: 0067-964X

from 2 to 11 mg kg^{-1}. These data constitute a characteristic signature of kimberlite zircons and are within a range of concentrations reported in the literature (Belousova et al., 2002). The analyzed crystals are marked by low concentrations of common Pb (≈8 mg kg^{-1}) and by high concentrations of U and total Pb, which allowed for high count rates and reliable statistics. The obtained values suggest that the Juína diamond field is composed of intrusions generated in two magmatic pulses (Fig. 11C).

Table 2. Summary of U/Pb and Lu-Hf data for the samples studied in this work.

Nº	Zircon	Age	Error	Epsilon Hf	TDM (Ga)
1	ZRJ-1	98.8	6.2	1.65 to 0.03	0.99 to 1.01
2	ZRJ-2	89	10	0.45 to -1.90	0.99 to 1.12
3	ZRJ-3	85.7	4.9	1.79 to -0.63	0.91 to 1.05
4	ZRJ-4	91	21	1.34 to -0.15	0.94 to 1.02
5	ZRJ-5	87.4	4.7	1.85 to -0.01	0.89 to 1.02
6	ZRJ-6	94.4	8.7	0.97 to -1.32	0.98 to 1.09
7	ZRJ-7	89	12	0.32 to -1.22	1.00 to 1.08
8	ZRJ-8	99.2	8	0.17 to -1.06	1.01 to 1.08
9	ZRJ-9	91.8	1.5	-0.48 to -1.76	1.06 to 1.10
10	ZRJ-10	85.5	4.3	0.31 to -1.65	1.04 to 1.11
11	ZRJ-11	95.8	3.7	0.09 to -1.87	1.02 to 1.12
12	ZRJ-12	84	15	2.87 to -1.19	0.89 to 1.08
13	ZRJ-13	89.4	0.73	1.60 to 0.05	0.92 to 1.02
14	ZRJ-14	85	17	1.65 to 0.03	0.93 to 1.01

The diagrams of Th/U versus number of analyzes (Fig. 11A) and $^{207}Pb/^{206}Pb$ ratio versus number of analyzes (Fig. 11B) indicate the existence of two distinct signature groups, consistent with the two U-Pb age groups (Fig. 11C). Thus, the results reported in this work allow us to suggest that occurred at least two pulses of kimberlite magmas in the Juína region distributed in time and with distinct Th and U concentrations.

The origin of the magmas that formed these megacrystals and the relationship of these crystals to kimberlite magma is an open discussion. Calculations of parental magma composition using empirical or experimental methods were documented by Jones (1987) and Moore et al. (1992). These authors consider that the modeling estimates are coherent only for the initial stages of fractionation, with the composition of magmas in the final stage being poorly characterized. According to Jones (1987), Sr and Nd isotopic data in clinopyroxene and garnet megacrystals indicate derivation from a source like ocean island basalt (OIB) magmas, with mean $^{87}Sr/^{86}Sr$ of 0.7035 and εNd of 12.5 to 14.7. The U-Pb method comprises older ages between the time the megacrystal formed in the mantle and its dragging into the kimberlite magma (Kinny et al., 1989).

boletim paranaense de Geociências
ISSN: 0067-964X

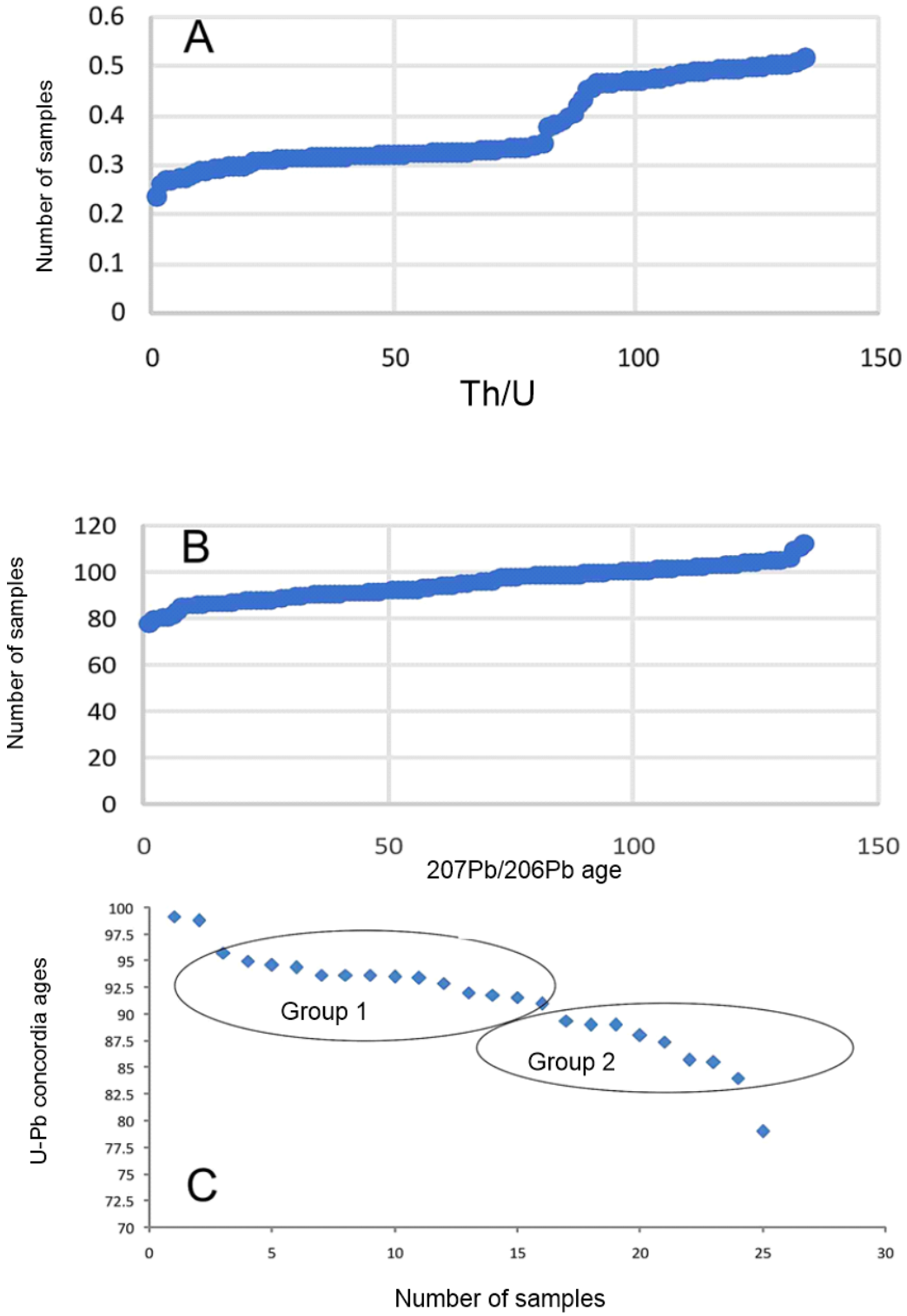

Figure 11. (A) Th/U diagram versus number of analyses; (B) 207Pb/206Pb ratio versus number of analyses. The diagrams indicate two groups of results suggesting two magma pulses.

boletim paranaense de Geociências
ISSN: 0067-964X

4.5 About the Hf isotopic composition of the lithospheric mantle in the Amazonian craton

The Subcontinental Lithospheric Mantle (SCLM) comprises a geochemical reservoir about six times larger than the mass of the continental crust (Griffin et al., 2000). The isotopic signatures of mantle extraction products indicate that the SCLM below the Precambrian cratons has existed for periods of time comparable to those of its crust (Richardson et al., 1984; Shirey and Walker, 1998; Carlson et al., 1999).

Estimates of SCLM composition, derived from xenoliths and xenocrysts in volcanic rocks (Griffin et al., 2000; 2002) show that SCLM composition is strongly correlated with the age of geological terrain formation. The composition of SCLM shows an evolution during geological epochs with meanhighly εHf depleted values in Archean cratonic roots, but they are relatively fertile in the Phanerozoic (Griffin et al., 2002), but with some examples of Archean SCLM enriched in incompatible elements (LREE, Zr and Sr), through metasomatic processes (Erlank et al., 1987). These observations indicate that the SCLM is not only a stable geochemical reservoir, but its composition is strongly correlated with its age.

Isotopic data are essential for understanding the processes that produced the variations in the composition of the SCLM. Higher values of Sr and Nd are available on xenoliths derived from the mantle of a small number of localities in Archean cratons, and a larger number on Phanerozoic crusts (e.g., Menzies, 1990). In contrast, few direct data are still available in the Lu-Hf system on SCLM samples, due in part to technical difficulties of sampling.

The zircon Lu-Hf isotopes are important tool to investigare the evolution of proto-kimberlite melts isince they represent megacrysts which are related to the SCLM origin. In this way, the isotopic composition of Hf in zircon grains from kimberlite rocks can provide important information to clarify the SCLM signatures. For this reason, to investigate the isotopic composition of the lithospheric mantle of the Amazonian craton, the Lu-Hf isotopic analyzes were performed for each zircon grain dated by U-Pb. The model ages obtained are between 1800 Ga and 1220 Ga and the εHf values varied between +1.90 and -1.81. These values found in the analyzed Juína zircon grains suggest that these kimberlite rocks were derived from an enriched mantle source. It is important to remember that all analyzed zircons have morphology typical of magmatic zircons even with the absence of crystal faces and have rounded shapes, probably due to chemical abrasion in the kimberlite magma (Kamenetsky et al., 2014).

According to Griffin et al. (2000), the hypothesis that the Hf isotopes may be enriched in the continental crust and depleted in the mantle (Blichert-Toft and Albarede, 1997) implies the existence of a third reservoir with a high Hf/Nd and non-radiogenic Hf. Metasomatic processes in the mantle are known to decouple large-ion lithophile elements (LILE) and *high field strength elements* (*HFSE*; Menzies, 1990; Hawkesworth et al., 1983; Griffin et al., 2000). Therefore, unusual Hf/Nd relationships in SCLM can be observed.

For example, zircon grains collected from kimberlites of different ages suggest a trend of isotopic evolution of Hf between the depleted mantle and the chondrite reservoir (Fig. 12). The study of zircon grains of Australian kimberlites (Timber Ckeek, Orroroo and Ptropus) show that in the Mesoproterozoic, the Ptropus kimberlite magma has negative εHf values, while Timber Kreek and Orrosoo kimberlites have positive values of εHf. In Russia, Archon and Proton kimberlites have positive εHf values, while Botswana kimberlites may have positive (Jwaneng kimberlite) or negative (Orapa and Monastery kimberlites) εHf values.

Zircon grains from Mbuji Mayi kimberlite, located in Archon Lunda-Kasai (Zaire or actual Democratic Republic of Congo), have εHf values between 5 and 8, while baddeleyite megacrystals from the same body provide εHf values from 15 to 10 (Fig. 15). These values

boletim paranaense de Geociências
ISSN: 0067-964X

are similar to those observed in the younger group of Jwaneng kimberlite zircons (Botswana), but the results indicate higher εHf values than most other Archean craton data.

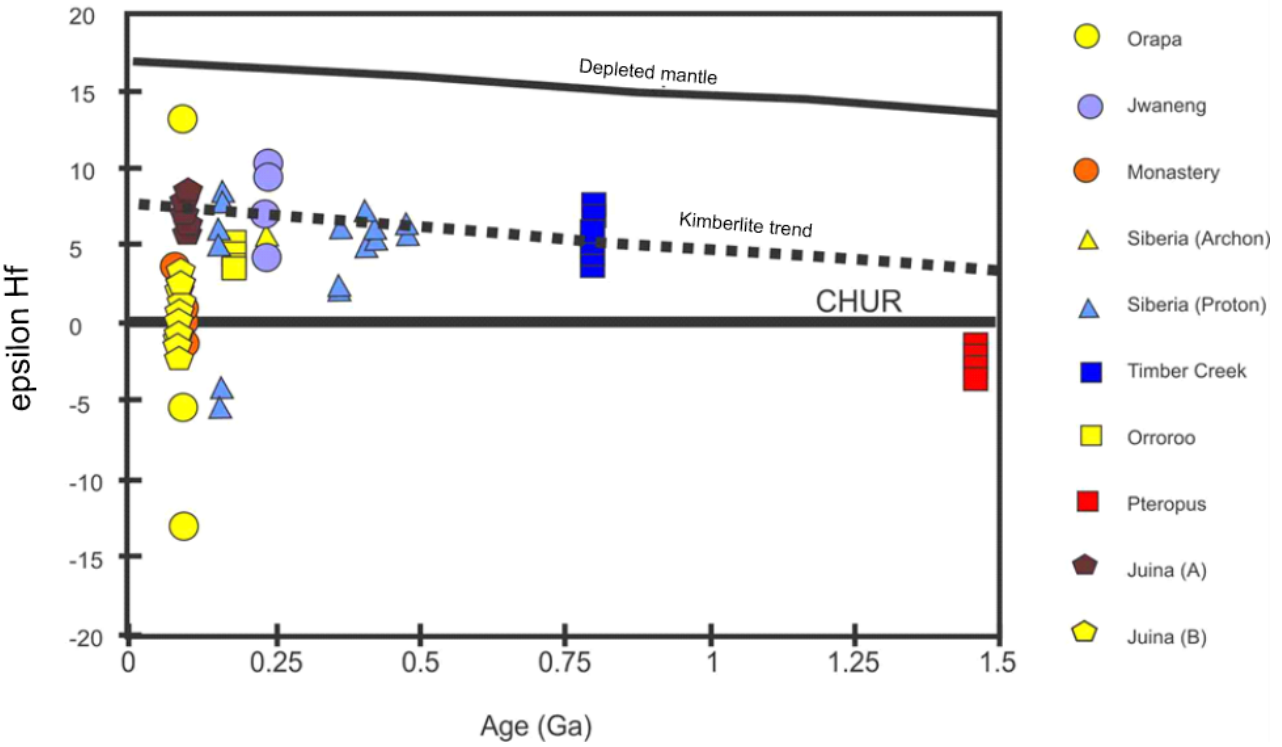

Figure 12. εHf values versus U-Pb ages found for the Juína kimberlite and literature data from literature on kimberlites.

Nowell and Pearson (1998) obtained εHf values between 5 and 2 in an ilmenite megacrystal from the Monastery mine. According to the authors, these values support the genetic linkage between the ilmenite and zircon megacrystals (Fig. 12). Analyzes of trace elements of ilmenite megacrystals in addition to εHf values, are important to clarify the relationships between the different sets of ilmenites, and their relationship to the zircons.

Kinny et al. (1989) reported SHRIMP analyzes of Hf isotopes in Jwaneng kimberlite (Botswana) zircon grains. Three grains from the youngest population provided $^{176}Hf/^{177}Hf$ values between 0.282866 and 0.283006. Two zircons from the older population provided ^{176}Hf /^{177}Hf values between 0.280416 and 0.280686. Several other kimberlite intrusions, such as Orapa, Jwaneng and Pteropus (South Africa), show wider ranges of εHf. These suites can represent zircons crystallized from a magma under assimilation process, fractional crystallization and reactions with the oldest lithosphere similar to the magma generator of the Monastery kimberlite, which display negative εHf values.

Recognition of two-age populations at Jwaneng (Botswana) and Timber Creek (Australian kimberlite) suggests that it is not possible to distinguish the mantle source (Kinny et al., 1989). As in the results of the zircon grains reported in this work, it seems reasonable to assume that the Hf isotopic reservoir of the SCLM of the Amazonian craton has a lower Hf epsilon signature than the magmas derived from the depleted mantle. Although this relation cannot be extended to other cratons, as demonstrated in the literature where examples of kimberlites with zircon grains with positive εHf values are reported.

The analyzed zircons of Juína (Mato Grosso state, Brazil) showed that the total concentrations of U and Th indicate the existence of two components in the magmas generated from the Juína kimberlite or through a magma that fractionated over time

boletim paranaense de Geociências
ISSN: 0067-964X

and generated products of different composition, as suggested by the existence of zircon grains with features that can originate in internal reactions that truncate the magmatic zonation (Fig. 13A and B). In addition, the εHf values and the model age are positive and negative (ranging from +2.9 to -2.9) and suggest a derivation of an enriched mantle source. These data constitute a characteristic signature of kimberlite zircons and are within a range of concentrations described in the literature.

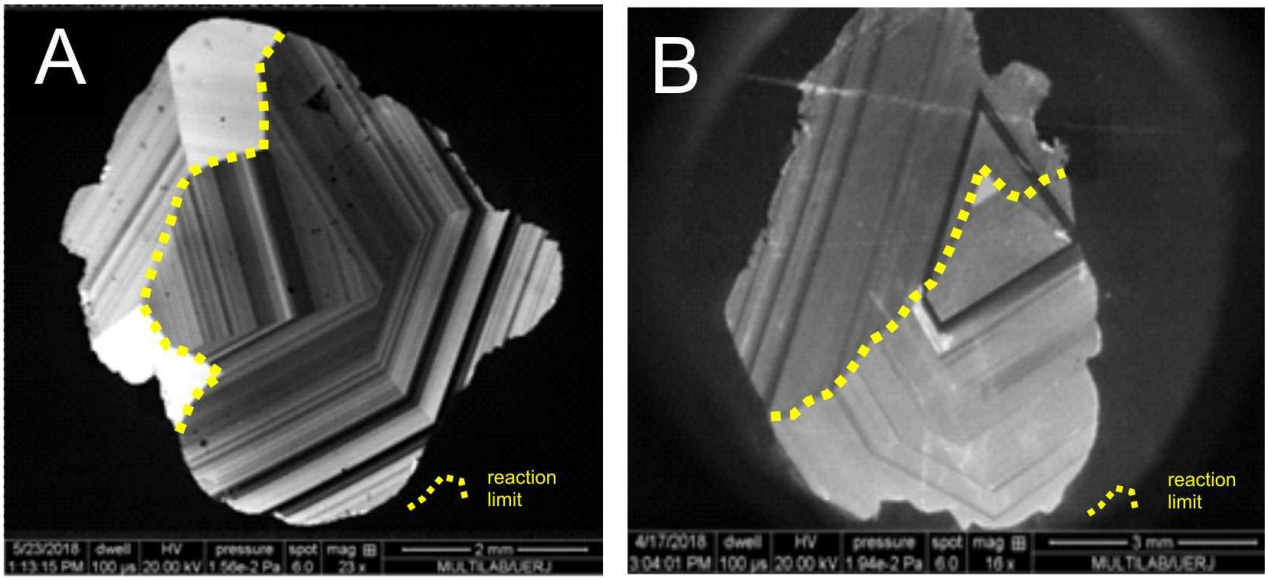

Figure 13. Zircon grains (A and B) with reaction edges that indicate magmatic evolution with zircon reabsorption and neoprecipitation.

5. CONCLUSION

The Juina kimbelite zircon grains present U-Pb ages obtained by LA-MC-ICP-MS from the concordia diagram are here interpreted as composed of two distinct groups: the first between 84 and 89 Ma and the second between 91 and 99 Ma. The zircon grains from the kimberlite province of Juína (Mato Grosso state, Brazil), studied in this work, have Hf isotopic compositions that are among the expected values for a chondritic reservoir, and magmas originated from a depleted mantle source. It can be argued that the zircon grains crystallized from proto-kimberlite magmas derived from a mantle source with variable depletion similar to those that produce OIB magmas (as indicated by ε_{Hf} values of up to 2.9) and enriched mantle sources. The low ε_{Hf} values of these zircon grains can be explained by several alternative models. A first explanation is the generation of megacrystal forming magmas within the lithosphere, which can occur as a result of the melting of a variety of reservoirs with different ages and wide variations of Hf isotopes. A second working hypothesis would be the crystallization of magmas generated from sources similar to reservoirs of composition type OIB (Ocean Island Basalts), but they were intruded into the lithosphere in several magmatic episodes over a long period of time of rock formation of the Rio Negro-Juruena province in the Amazonian craton. It can also be hypothesized that depleted mantles that interacted with non-radiogenic Hf reservoirs in the lithosphere.

ACKNOWLEDGMENT

The authors would like to thank the Conselho Nacional de Desenvolvimento Científico e Tecnológico of Brazil, CNPq (processes #302676/2019-8 to MVAM; and #301470/2016-2 to MCG) and Fundação Carlos Chagas Filho de Amparo à Pesquisa do Estado do Rio de Janeiro, FAPERJ (processes: E-26/202.927/2019 to MVAM; E-26/202.843/2017 to MCG) Brazil, for financial support.

boletim paranaense de Geociências
ISSN: 0067-964X

REFERENCES

ALMEIDA, F. F. M. DE, HASUI, Y., BRITO NEVES, B. B. DE, & FUCK, R. A. (1981). Brazilian structural provinces: an introduction. Earth-Science Reviews, 17 (1-2), 1-29.

AMELIN, Y., LEE, D.C., HALLIDAY, A.N. 2000 Early-middle Archean crustal evolution deduced from Lu–Hf and U–Pb isotopic studies of single zircon grains, Geochim. Cosmochim. Acta 64 () 4205–4225.

AMELIN, Y., LEE, D.C., HALLIDAY, A.N., PIDGEON, R.T., 1999 Nature of the Earth's earliest crust from hafnium isotopes in single detrital zircons, Nature 399, 252– 255.

ANDERSEN, T. GRI,FFIN, W.L., PEARSON, N.J., 2002 Crustal evolution in the SW part of the Baltic Shield: the Hf isotope evidence, J. Petrol. 43, 1725–1747.

BELOUSOVA E.A., GRIFFIN W.L., O´REILLY S., FISHER N.I. 2002. Igneous zircon: trace elements composition as an indicator of source rocks type. Mineralogy and Petrology, 143(5):602-622.

BODET, F., SCHARER, U. 2000 Evolution of the SE-Asian continent from U–Pb and Hf isotopes in single grains of zircon and baddeleyite from large rivers, Geochim. Cosmochim. Acta 64 () 2067– 2091.

BRITO NEVES, B.B., TEXEIRA, W., TASSINARI, C.C.G., KAWASHITA, K., 1990. A contribution to the subdivision of the Precambrian in South America. Revista Brasileira de Geociências 20 (1–4), 267–276.

CORDANI, U.G., TEIXEIRA, W., 2007. Proterozoic accretionary belts in the Amazonian Craton. In: HatcherJr. Jr., R.D., CARLSON, M.P., MCBRIDE, J.H., MARTÍNEZ CATALÁN, J.R. (EDS.), 4-D Framework of Continental Crust: Geological Society ofAmerica, Memoir No. 200, pp. 297–320.

CORFU, F., HANCHAR, J. M. HOSKIN P. W. O AND KINNY, P. 2003 "Atlas of Zircon Textures," Reviews in Mineralogy & Geochemistry, Vol. 53, No. 1, pp. 469-500. doi:10.2113/0530469

COSTA, V.S. 7 GSPAR, J.C. 2001 Intercrecimento gráfico ilmenita-pclinopiroxenio em nodulos de jimberlito de Juína, MT: petrografia e quimica mineral. Revista Brasiçeira de Geociencias, 31(4):569-574.

DAVIS D.W., WILLIAM I.S. &KROGH T.E. 2003. Historical Development of Zircon Geochronology. In: Hanchar, J.M. & Hoskin, P.W.O. (Eds.). Reviews in Mineralogy and Geochemistry: Zircon. Mineralogical Society of America, 53:145-181.

DAVIS, G.L. 1977. The Age of Uranium Contents of Zircons from Kimberlites and Associated Rocks. In: F.R. Boyd& H.O.A. MEYER (Eds.) Proc. 2 intern. Kimberlite Conf., Ext. abs., 67-69.

ELHLOU, S., BELOUSOVA, E., GRIFFIN, W.L., PEARSON, N.J. AND O'REILLY, S.Y., 2006. Trace element and isotopic composition of GJ-red zircon reference material by laser ablation. Goldschmidt Conference abstracts, A-5.Formoso M.L.L., TRESCASSES J.J., DUTRA C.V. & GOMES C.B. (coord.) 1984. Técnicas analíticas instrumentais aplicadas à geologia. São Paulo, Editora Edgard Blücher, 218 pp.

GERALDES, M.C. 2010 Introdução à geocronologia. São Paulo: Sociedade Brasileira de Geociências,

GOLDMANN, A., G. BRENNECKA, J. NOORDMANN, S. WEYER, AND M. WADHWA. 2015. "The Uranium Isotopic Composition of the Earth and the Solar System." Geochimica et Cosmochimica Acta 148: 145–158.

GRIFFIN, W.L., PEARSON, N.J., BELOUSOVA, E., JACKSON, S.E., VAN ACHTERBERGH, E., O'REILLY, S.Y., SHEE, S.R., 2000 The Hf isotope composition of cratonic mantle: LAM-MC-ICPMS analysis of zircon megacrysts in kimberlites, Geochim. Cosmochim. Acta 64, 133–147.

GRIFFIN, W.L., WANG, X., JACKSON, S.E., PEARSON, N.J., O'REILLY, S.Y., XU, X., ZHOU, X., 2002 Zircon chemistry and magma mixing, SE China: in-situ analysis of Hf isotopes. Tonglu and Pingtan igneous complexes, Lithos 61, 237– 269.

GÜNTHER D. & HATTENDORF B. 2005. Solid sample analysis using laser ablation inductively coupled plasma mass spectrometry. Trends Anal. Chem., 24: 255-265.

HAWKESWORTH C. & KEMP T. 2006. Using hafnium and oxygen isotopes in zircons to unravel the record of crustal evolution. Chem. Geol., 226: 144-162.

HEAMAN, L., TEIXEIRA, N.A., GOBBO, L. & GASPAR, J.C. 1998. U-Pb mantle zircon ages for kimberlites from the Juína and Paranatinga provinces, Brasil. Proceedings of the 7th International Kimberlite Conference, Cape Town. Ext. Abs., p.322-324.

HOLMES, A. A 1947. Revised Estimate of the Age of the Earth. Nature 159, 127–128.

HOUTERMANS, F. G., 1946. The isotope ratios in natural lead and the age of uranium, Naturwissenschaften, 33, 185.

JACKSON, S. E., PEARSON, N. J., GRIFFIN, W. L., & BELOUSOVA, E. A. (2004). The application of laser ablation-inductively coupled plasma-mass spectrometry to in situ U-Pb zircon geochronology. Chemical Geology, 211(1–2), 47–69.

KAMENETSKY, VADIM & BELOUSOVA, ELENA & GIULIANI, ANDREA &KAMENETSKY, MAYA &GOEMANN, KARSTEN & GRIFFIN, WILLIAM. (2014). Chemical abrasion of zircon and ilmenite megacrysts in the Monastery kimberlite: Implications for the composition of kimberlite melts. Chemical Geology. 383. 76–85. 10.1016/j.chemgeo.2014.06.008.

KAMINSKY, F. V., SABLUKOV, S. M., BELOUSOVA, E. A., ANDREAZZA, P., TREMBLAY, M., & GRIFFIN, W. L. (2010). Kimberlitic sources of super-deep diamonds in the Juína area, Mato Grosso State, Brazil. Lithos, 114(1–2), 16–29. https://doi.org/10.1016/j.lithos.2009.07.012.

KINGSTON, D.R.; DISHROON, C.P.; WILLIAMS, P.A., 1983. Global basin classification system. American Association of Petroluem Geologists Bullentin, v. 67, p. 2175-2193.

KINNY P.D. & MAAS R. 2003. Lu–Hf and Sm–Nd isotope systems in zircon. In: Hanchar J.M., Hoskin P.W.O. (eds.) Zircon. Reviews in Mineralogy and Geochemistry. Mineralogical Society of America, 53, Washington, DC, p.: 327-341.

KINNY, P.D., COMPSTON, W., WILLIAMS, I.S., 1991 A reconnaissance ion probe study of hafnium isotopes in zircons, Geochim. Cosmochim. Acta 55, 849– 859.

KLEIN, G.V. 1995. Intracratonic Basins. In: Busby, C.J.; Ingersoll, R.V. (eds.). Tectonics of Sedimentary Basins. Cambridge: Blackwell Science, p. 459-478.

Marzolli, A.; Renne, P.R.; Picirillo, E.M.; Ernesto, M.; Belliene, G.; MIN, A. ,1999. Extensive 200 million-year-old continental flood basalts of the Central Atlantic Magnatic Province. Science, n. 284, p. 616-618.

MELO, D.P. & FRANCO, M.S.M.,1980. Geomorfologia. In: Brasil. Ministério das Minas e Energia. Projeto RadamBrasil. Folha SC.21- p.117-162.

MOREL, M.L.A., NEBEL, O., NEBEL-JACOBSEN, Y.J., MILLER, J.S., VROON, P.Z. 2008. Hafnium isotope characterization of the GJ-1 zircon reference material by solution and laser-ablation MC-ICPMS. Chemical Geology, 255: 231–235.

boletim paranaense de Geociências
ISSN: 0067-964X

NOWELL, G.M.., PEARSON, D.G., BELL, D.R., CARLSON, R.W., SMITH, C.B., KEMPTON, P.D., NOBLE, S.R., 2004 Hf isotope systematics of kimberlites and their megacrysts: new constraints on their source regions. J. Petrol., 45 (8), pp. 1583-1612

NANNINI, F., NETO, I.C., VALDIR SILVEIRA, F.V., CUNHA, L.M., OLIVEIRA, R.G., WESKA, R.K. ET AL., 2017. Áreas kimberlíticas e diamantíferas do Estado do Mato Grosso. Ministério De Minas E Energia Secretaria De Geologia, Mineração E Transformação Mineral Serviço Geológico Do Brasil – CPRM, Diretoria de Geologia E Recursos Minerais, Departamento de Recursos Minerais, Programa Geologia do Brasil, Informe de Recursos Minerais, Série Pedras Preciosas, nº 12, Informe de Recursos Minerais Complementar ao Mapa das Áreas Kimberlíticas e Diamantíferas do Estado do Mato Grosso. Escala 1:1.000.000, Brasília.

NEBEL O., NEBEL-JACOBSEN Y., MEZGER K., BERNDT J. 2007. Initial Hf isotope compositions in magmatic zircon from early Proterozoic rocks from the Gawler Craton, Australia: A test for zircon model ages. Chem. Geol., 241: 23-37.

PATCHETT, P. J. AND TATSUMOTO,M., 1980. Hafnium isotope variations in oceanic basalts. Geophys Res Lett 7: 10771080.

PATCHETT P. J. AND TATSUMOTO M. (1981). Lu/Hf in chondrites and definition of a chondritic hafnium growth curve. Lunar Planet. Sci. 12, 822) 4, Lunar Planet. Inst.

PATCHETT, P.J. KUOVO, O., HEDGE, C.E., TATSUMOTO, M., 1981 Evolution of the continental crust and mantle heterogeneity: evidence from hafnium isotopes, Contrib. Mineral. Petrol. 78 279– 297.

PEDREIRA, A.J. & BAHIA, R.B.C., 2004. Estratigrafia e evolução da Bacia dos Parecis. Região Amazônica, Brasil. Integração e síntese de dados dos projetos Alto Guaporé, Serra Azul, Serra do Roncador, Centro Oeste de Mato Grosso e Sudeste de Rondônia. Brasília: CPRM.

PUPIN J.P. 1980. Zircon and granite petrology. Mineralogy and Petrology, 73: 207 – 220.

RIETVELD, H.M. A profile refinement method for nuclear and magnetic structures. J. Appl. Cryst., n.2, p.65-71, 1969.

RUBATTO D. & HERMANN J. 2003.Zircon formation during fluid circulation in eclogites (Monviso, Western Alps): Implications for Zr and Hf budget in subduction zones. Geochimica et Cosmochimica Acta, 67: 2173-2187.

RUSSO R.E., MAO X.L., LIU H., GONZALEZ J., MAO S.S. 2002. Laser ablation in analytical chemistry – a review. Talanta, 57: 425-451.

SABEDOT, S. E SAMPAIO, C. H. (2002). Caracterização de zircões da Mina Guaju (PB). Rev. Esc. Minas, vol 55, no 1, UFOP.

SANTOS, J.O.S., HARTMANN, L.A., GAUDETTE, H.E., GROVES, D.I., MCNAUGHTON, N.J., FLETCHER, I.R., 2000. A new understanding of the provinces of the Amazon Craton based on integration of field mapping and U-Pb and Sm-Nd geochronology. Gondwana Res. 3, 453-488.

SCANDOLARA, J.E., CORREA, R.T., FUCK, R.A., SOUZA, V.S. RODRIGUES, J.B. RIBEIRO, P.S.E., FRASCA, A.A.S. SABOIA, A.M., LACERDA FILHO, J.V., 2017. Paleo-Mesoproterozoic arc-accretion along the southwestern margin of the Amazonian craton: The Juruena accretionary orogen and possible implications for Columbia supercontinent. Journal of South American Earth Sciences 73, 223-247.

SCHERER, E., CARSTEN, M., MEZGER, M., 2001. Calibration of the lutetium – hafnium clock. Science 293, 683 – 687.

SILVEIRA, F.V. Potencial para exploração de diamantes no Brasil. Acessado Somexmin 2016. em http://www.adimb.com.br/simexmin2016/palestra/auditorio_sao_joao_delrey_17/9h50%20Francisco%20Silveira.pdf

Siqueira L.P. 1989. Bacia dos Parecis. Boletim de Geociências da Petrobrás, 3:3-16.

SLÁMA J., KOŠLER J., CONDON D.J., CROWLEY J.L., GERDES A., HANCHAR J.M., HORSTWOOD M.S.A., MORRIS G.A., NASDALA L., NORBERG N., SCHALTEGGER U., SCHOENE B., TUBRETT M.N., WHITEHOUSE M.J. 2008. Plešovice zircon – a new natural reference material for U–Pb and Hf isotopic microanalysis. Chem. Geol., 249: 1-35.

STEIGER, R.H., AND JAEGER, E., 1977, Subcommission on geochronology: Convention on the use of decay constants in geo- and cosmochronology: Earth Planetary Science Letters, v. 36, p. 359–362

TAKEHARA L., HARTMANN L.A., VASCONCELLOS M.A.Z., SUITA M.T.F. 1999. Evolução magmática e metamórfica de zircão do complexo Barro Alto (GO), com base em imagens de elétrons retro-espalhados e análises químicas por microssonda eletrônica. Revista Brasileira de Geociências29: 371-378.

TASSINARI C.C.G., CORDANI U.G., NUTMAN A.P., VAN SCHMUS W.R., BETTENCOURT J.S., TAYLOR P.N. 1996. Geochronological systematics on basement rocks from the Rio Negro-Juruena Province and tectonic implications. International Geology Review, 38:1161-1175.

TASSINARI, G.G., MACAMBIRA, M.J.B., 1999. Geochronological provinces of the Amazonian Craton. Episodes 22, 174–182.

TEIXEIRA, N.A. GASPAR, J.C. OLIVEIRA, A.L.A.M., BITENCOURT, R.M., YEDA, B. 1998a. Morphology of the Juínamaars. In: 7th Intern. Kimberlite Conf., Ext. Abstp. 902-904.

TEIXEIRA, N.A. GASPAR, J.C. WAISSEL, O., ALMEIDA, J.A., GOBBO L. I998b. Geology ofthe Juína diamantiferous province. In : 71thIntern. Kimberlite Conf., Ext. Abst p. 905-907.

TEIXEIRA, W.; TASSINARI, C. C. G.; CORDANI, U. G.; KAWASHITA, K. 1989 A review of the geochronology of the Amazonian Cráton: tectonic implications. Precambrian Research, v. 42, p. 213-227.

THIRLWALL, M.F., WALDER, A.J., 1995 In situ hafnium isotope ratio analysis of zircon by inductively coupled plasma multiple collector mass spectrometry, Chem. Geol. 122, 241–247.

TISSOT, F. L. H., AND N. DAUPHAS. 2015. “Uranium Isotopic Compositions of the Crust and Ocean: Age Corrections, U Budget and Global Extent of Modern Anoxia.” Geochimica et Cosmochimica Acta 167: 113–143.

VAN DER LEE, S., JAMES D., SILVER, P., 2001. Upper-mantle S-velocity structure of central and western South. America. Journal of Geophysical Research, Vol. 106 (12), 30,821-30,835. DOI: 10.1029/2001JB000338

WETHERHILL, G.W., 1956, Discordant uranium-lead ages I: American Geophysical Union Transactions, v. 37, p. 320–326.

WIEDENBECK, M., ALLE´, P., CORFU, F., GRIFFIN, W.L., MEIER, M., OBERLI, F., VON QUADT, A., RODDICK, J.C., SPIEGEL, W., 1995. Three natural zircon standards for U–Th–Pb, Lu–Hf, trace element and REE analyses. Geostand. Newsl. 19, 1–2.

XIE L.W., EVANS N., YANG Y.H., HUANG C. AND YANG J.H. (2018) U-Th-Pb geochronology and simultaneous analysis of multiple isotope systems in geological samples by LA-MC-ICP-MS. Journal of Analytical Atomic Spectrometry, 33, 1600– 1615.

Submetido em 24/11/2021
Aceito em 26/10/2022